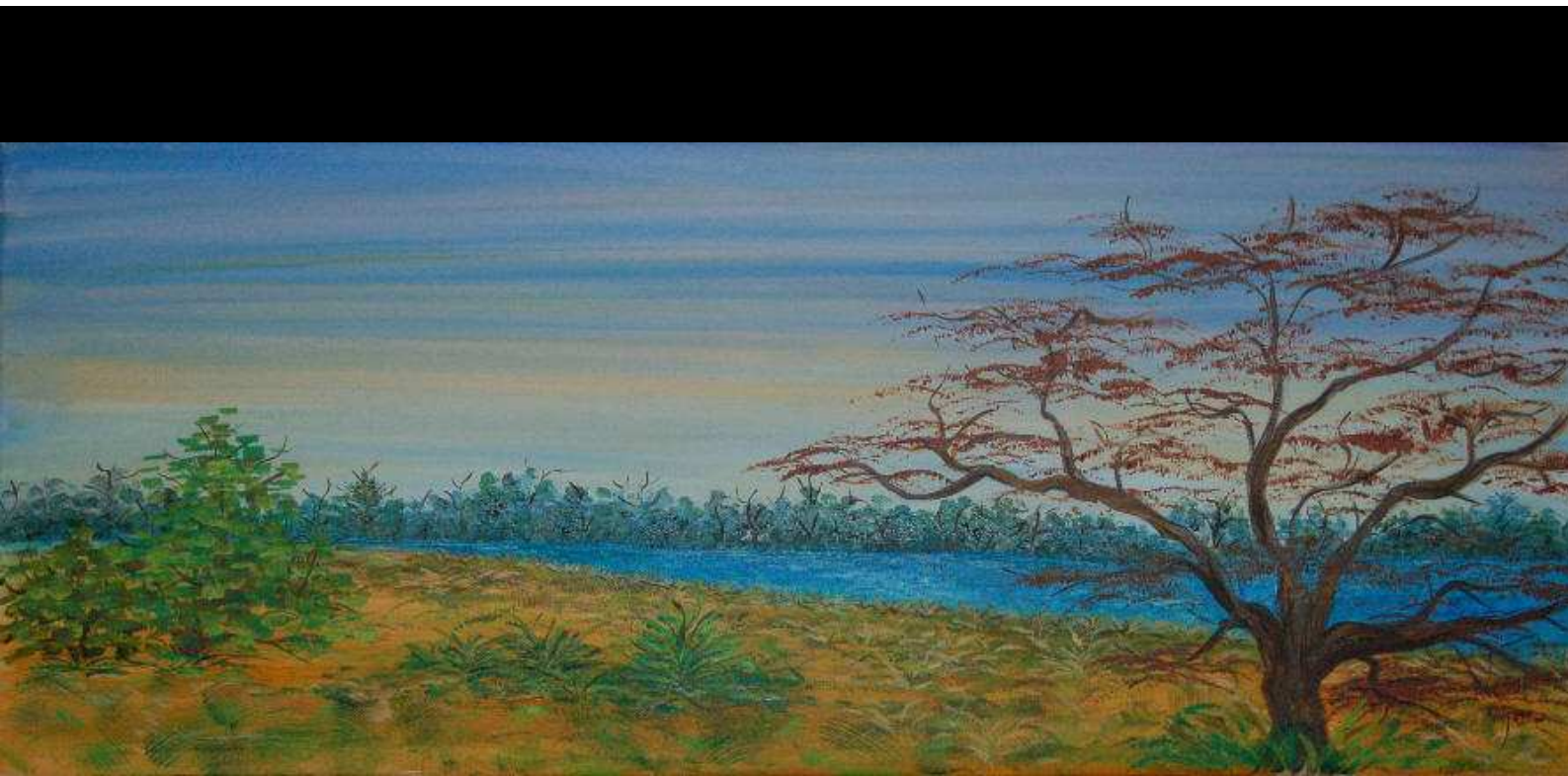


Soil salinization on the floodplains of the Lower Shire River

Bachelor thesis



Jorick Velema
Enschede, 19 December 2008

Soil salinization on the floodplains of the Lower Shire River

Bachelor thesis

Enschede, 19 December 2008

This thesis is a research on the processes of soil salinization on the floodplains of the Lower Shire River, Malawi. It is part of the Bachelor program Civil Engineering (&Management), University of Twente, the Netherlands.

Jorick Velema
Bachelor student University of Twente
s0077585

Supervisor of the University of Twente, The Netherlands
Dr. ir. D.C.M. Augustijn
Faculty of Engineering Technology, department of Water Management

Supervisor of the University of Oslo, Norway
Professor P. Aagaard
Department of Geosciences

Albert Einstein:

*“If we knew what it was we were doing,
it would not be called research, would it? “*

Preface

This report is the result of a three month internship at the University of Oslo, Department of Geosciences, Norway. The internship is part of the Bachelor program Civil Engineering of the University of Twente, the Netherlands. My stay in Norway was a great experience for me. The life in Oslo, the people and the beautiful environment of Norway. During my stay I met a lot of new friends from different countries. Not taking any courses, but actually doing a “real” research was new to me, but in the end a positive experience.

The out come of this research was open at the start. There was no precise description of the assignment, almost no data was available and within the time scope of three months there was no possibility to visit the study area myself. This resulted in a short research strategy which was filled in during the actual research. The lack of data was filled with available data from literature. At some points the research strategy was adjusted to the data available. Because there was no precise description of the assignment I had a lot of freedoms. This gave me the opportunity to use my own sighs and creativity but also the dilemma “what if it does not work out”.

The decision to create a numerical model was born because I did not have the available data and time to use an existing model. Creating the model in Matlab was challenging and a process from which I learned a lot. On the other hand was it a risk because I had no idea if the model would work and give me results which could be used for the research. I am moderately satisfied with the results of the model but grateful that I had the chance to learn much about water flows in the unsaturated zone and modeling.

I like to thank professor Per Aagaard and professor Lena Tallaksen for the possibility to perform my Bachelor thesis at the department of Geosciences and their help during my internship. I would also like to thank dr. ir. Denie Augustijn for his support from the Netherlands and his correction in my concept report. Last I would like to thank Ms Ellen van Oosterzee-Nootenboom for her help finding a proper bachelor assignment.

Enschede, December 2008

Jorick Velema

Summary

The floodplains of the Lower Shire River are one of the seventeen major floodplains in Africa and directly benefit an estimated 1 million people in riparian communities in Malawi and Mozambique. Certain areas of the floodplains exposed to flooding are experiencing soil salinization. Objective of the research is to determine if the soil salinization is caused by flooding or by capillary action, by performing a literature study and setting up a 1D soil water model.

Malawi is a land-locked country located in south-east Africa lying along a sector of the East African Rift. The biggest lake, Lake Malawi, drains freely into the Indian Ocean through the Shire River then the Zambezi. The Shire River is the only outlet from Lake Malawi from which it meanders southwards for a distance of approximately 700 km to its confluence with the Zambezi River.

The floodplains of the Lower Shire River studied in the research floods every year when the water level in the Shire River rises. After the floods water stays behind on the floodplains which infiltrates and evaporates. Under the floodplains are two aquifers. A unconfined saline aquifer (3779 mg/L sodium) with a groundwater level of 0,5 m and a confined fresh water aquifer starting at 20m below surface. The climate of the Lower Shire Valley is characterized by two well-defined seasons; the hot-dry season from May to October, and the warm-wet season from November to April. The precipitation is 788mm/year and the evaporation is 2080mm/year making the valley evaporation dominated.

To study to the soil salinization, the different processes that influence the soil salinization are simulated in a 1D numerical model. Any process that affects the soil-water balance may affect the movement and accumulation of salts in the soil. These processes include; hydrology, climate, irrigation, drainage, plant cover and rooting characteristics, farming practices. Two possible soil salinization processes might occur. This is soil salinization due to flooding and soil salinization due to capillary rise.

The unsaturated water flow is calculated with Richards Equation. The solute movement is simplified to an advective flux only. Both Richards Equation and the solute movement are discretized. The discretizations are programmed in Matlab together with the other processes. The hydraulic conductivity and the pressure head have been determined by the relation suggested by Campbell (1974).

Four simulations representing the floodplains of the Lower Shire River are performed. From these simulations can be concluded that the soil salinization is caused by capillary rise. The average salt accumulation calculated in the model is 5,9 kg/m² sodium chloride. From a graph where the total salt accumulation is plotted as a function of the groundwater depth and a graph where the total salt accumulation is plotted as a function of the effective evaporation it can be concluded that the model holds errors though.

These errors might be caused by a various different reasons. Most likely the errors are caused by errors in the relations suggested by Campbell (1974), instability, evaporation or the constant groundwater level. Also the simplification of the solute movement could causes errors in the total salt accumulation. With more study the performance of the model could be increased greatly, and eventually it can be used to make real estimations of soil salinization.

Table of contents

Preface.....	4
Summary	5
Table of contents	6
Table of figures	8
1. Introduction	9
2. Study Area.....	11
2.1. Malawi.....	11
2.2. Lower Shire River	11
2.3. Climate of the Lower Shire Valley	12
2.3.1. Precipitation	12
2.3.2. Air temperature	13
2.4. Hydrograph of the Lower Shire River.....	13
2.5. Floodplains Lower Shire River	14
2.5.1. Soil of the floodplains	14
2.5.2. Aquifers and salinity	15
3. Soil salinization processes.....	16
3.1. Soil Salinization due to flooding.....	16
3.2. Soil Salinization due to capillary rise.....	16
4. One dimensional soil water model	17
4.1. Basics of the model	17
4.1.1. Model assumptions.....	17
4.1.2. Unsaturated water flow	17
4.1.3. Solute movement.....	18
4.1.4. Evaporation	19
4.1.4.1. Free-water evaporation.....	19
4.1.4.2. Bare soil evaporation.....	20
4.2. Model	21
4.2.1. Model stages.....	21
4.3. Model configuration	22
4.3.1. Delta t and delta x.....	22
4.3.2. Maximum sodium concentration.....	22
4.3.3. Duration of simulation	23
5. Results	24
5.1. Run 1: sandy clay and 0,4 m surface water.....	24
5.2. Run 2: sandy clay and 0,15 m surface water.....	25
5.3. Run 3 and 4	26
5.4. Influence of groundwater level	26
5.5. Influence of effective evaporation.....	26
6. Discussion	28

6.1. Errors types	28
7. Conclusion.....	29
8. References	30
Appendix I, Map of the Lower Shire Valley	33
Appendix II, Climate data.....	34
II.1. Windspeed.....	34
II.2. Cloud cover	34
II.3. Water temperature	34
II.4. Relative humidity	35
II.5. Rainfall	36
Appendix III, Numerical discretizations	37
III.1. Discretization Darcy's Law and Richards equation.....	37
III.2. Discretization solute movement	38
Appendix IV, Shortwave and longwave radiation	40
IV.1.1.1. Shortwave radiation.....	40
IV.1.1.2. Longwave radiation.....	41
Appendix V, Results run 3 and 4	43
Appendix VI, Matlab script.....	44

Table of figures

Figure 1, Salt deposition on the floodplains of the Lower Shire River, photo R.Vogt, University of Oslo.....	9
Figure 2, Salt extraction from soil, photo R.Vogt, University of Oslo	9
Figure 3, Maps of Malawi	11
Figure 4, Lower Shire River, located down stream from Chikwawa	12
Figure 5, panorama photo of the floodplains of the Lower Shire River.....	12
Figure 6, Mean monthly precipitation Lower Shire Valley.....	13
Figure 7, Mean monthly air temperature of the Lower Shire Valley, data based on measurements by Chimatiro (2004)	13
Figure 8, Hydrograph of the floodplain of the Lower Shire River, at Chikwawa.....	14
Figure 9, Floodplain flooding and drying process.....	14
Figure 10, Profile of aquifers	15
Figure 11, Soil salinization due to flooding	16
Figure 12, Soil salinization due to capillary rise	16
Figure 13, Mean monthly evaporation from surface water.....	20
Figure 14, Model input, processes and output	21
Figure 15, water flow in the unsaturated zone, run 1	24
Figure 16, sodium concentration and salt accumulation, run 1.....	24
Figure 17, water flow in the unsaturated zone, run 2	25
Figure 18, sodium concentration and salt accumulation, run 2.....	25
Figure 19, total salt accumulation as a function of the groundwater depth	26
Figure 20, total salt accumulation as a function of the effective evaporation	27
Figure 21, The Lower Shire Valley of Nyasaland	33
Figure 22, Mean monthly wind speed, data based on measurements by Chimatiro (2004)	34
Figure 23, Mean monthly cloud cover, data based on measurements Chimatiro (2004)	34
Figure 24, Mean monthly water temperature, data based on measurements Chimatiro (2004)	34
Figure 25, Mean monthly relative humidity, data received from the Department of Meteorological Services, Ngabu 1972-2006.....	35
Figure 26, Numerical scheme unsaturated water flow.....	37
Figure 27, Numerical scheme solute movement	38
Figure 28, Mean monthly clearness index of the Shire Valley	40
Figure 29, Mean monthly daily extraterrestrial radiation of the Shire Valley	41
Figure 30, Mean monthly daily shortwave radiation of the Shire Valley	41
Figure 31, Mean monthly daily longwave radiation of the Shire Valley.....	42
Figure 32, water flow in the unsaturated zone, run 3	43
Figure 33, sodium concentration and salt accumulation, run 3.....	43
Figure 34, water flow in the unsaturated zone, run 4	43
Figure 35, sodium concentration and salt accumulation, run 4.....	43

1. Introduction

Soil salinization is an important worldwide environmental problem. The analysis of soil salinization has long played a crucial role in environmental sciences. Salinity can negatively influence soil quality as it can threaten the biodiversity, rural and urban infrastructure, water quality and agricultural production (Wang, Xiao, Li, & Li, 2007).

Soluble salts are a natural feature of the landscape, being present usually in small amounts in all waters, soils and rocks (Yaalon, 1967). Under certain conditions these salts can accumulate in the soil, a process called soil salinization (Schofield, Thomas & Kirkbu, 2001). Salt accumulates when mineralized water at or near the ground surface continually evaporates and causes minerals to precipitates. This can be due to evapotranspiration, hydrolysis and leakage between aquifers (Salama, Otto & Fitzpatrick, 1999). Soil salinization is closely related to surface soil and ground water hydrological processes, as the movement of water is mainly responsible for the transport of salt (Xu, Shao, 2002). These processes include; hydrology, climate, irrigation, drainage, plant cover and rooting characteristics, farming practice (The U. S. Department of Agriculture, 1998). Salts accumulate by primary (natural) processes and secondary (human influenced) processes (Schofield, Thomas & Kirkby, 2001). The main determinants of natural salinization are climatic, oceanic, topographic and geological factors. Some of the main causes of secondary salinization are irrigation, deforestation, afforestation and river impoundment (Schofield et al, 2001).

The floodplains of the Lower Shire River is one of the seventeen major floodplains in Africa and directly benefits an estimated 1 million people in riparian communities in Malawi and Mozambique (Chimatiro, 2004). The floodplains of the Lower Shire Valley are an important habitat for wildlife and for crop production (rice, cotton, beans, sorghum, millets and sugar cane) (Chimunthu Banda 2008). Certain areas exposed to flooding experience soil salinization. Salt deposits have occurred naturally in these areas for several decades in the top part of the soil, see figure 1. Excessive salinity leads to toxicity in crops and reduction of the available water to crops by reducing the osmotic potential of the soil solution (Hillel, 1980), making the soil unsuitable for crop farming. In places where the salts accumulate no plants tend to grow, these parts of the floodplains consist of bare soil, see figure 1.



Figure 1, Salt deposition on the floodplains of the Lower Shire River, photo R.Vogt, University of Oslo



Figure 2, Salt extraction from soil, photo R.Vogt, University of Oslo

Currently, in some parts of the floodplains of the Lower Shire River, people are traditionally engaged in small scale salt production from saline soils. To extract the salt the top-soil is scraped off by the villagers and the salt is then extracted by a locally derived but somewhat primitive process, figure 2. According to Malawi Industrial Research and Technology Development Centre (2000) the salt rises to the surface of the soil through capillary action and forms a thin layer on the ground. The local people believe the salt accumulates from the floodwater on to the top layer of the soil.

Goal of the research is to determine if the soil salinization on the Floodplains of the Lower Shire River is caused by flooding or by capillary action, by performing a literature study and setting up a 1D soil water model.

The research exists of two stages. First stage is a literature study to gather knowledge about the processes behind soil salinization and data of the Shire Valley. Second stage is to apply the results from the literature study into a numerical 1D soil water model. Many models are available to simulated unsaturated groundwater flow and soil salinization. These models need a lot of input data which is not available for the floodplains of the Lower Shire River. Also within the time scope of three months there is not enough time to learn and work with an existing model. To simulate the soil salinization a simple numerical model is set up based on the available data and knowledge gather in the literature study. The model is written and run in Matlab and holds the basics of the groundwater flow in the unsaturated zone. With the model an estimation is made on the amount of salt that accumulates and its source.

The research is part of a NUFU project “Capacity Building in Water Sciences for Improved Assessment and Management of Water Resources”. NUFU is the Norwegian Cooperation Program for Development, Research and Higher Education. The NUFU program is a program for independent academic cooperation based on initiatives from researchers and institutions in the South and their partners in Norway. The project “Capacity Building in Water Sciences for Improved Assessment and Management of Water Resources” is a collaborative network research project between The University of Malawi, University of Oslo, the University of the Western Cape and University of Botswana. The overall goal of the project is to improve human welfare among the resource poor through improved access and availability of wholesome and safe water (Vogt, 2008). The research is an initiative of the local people that farm salt on the floodplains of the Lower Shire River, who would like to know more about the source and process of the soil salinization.

The thesis contains seven chapters. Chapter two contains the study area, the Lower Shire Valley. In chapter three the Soil salinization processes are described. Chapter four contains the numerical model. The results of the model are presented in chapter five. Last chapters of this thesis, chapter six and seven, contain respectively the discussion and the conclusion.

2. Study Area

The area of interest in this research is the Lower Shire Valley in Malawi. This chapter describes the different layers of the study area; Malawi, the Lower Shire River, climate of the Lower Shire River, hydrograph of the Lower Shire River and the Floodplains of the Lower Shire River.

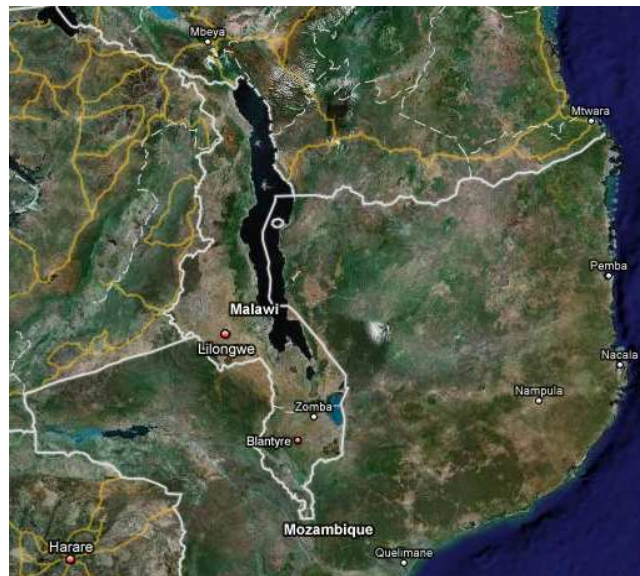
2.1. Malawi

Malawi is a land-locked country located in south-east Africa lying along a sector of the East African Rift Valley between latitudes 9° and 18° S, and longitudes 33° and 36° E. It is boarded by Tanzania in the north and north-east, Zambia in the west, and Mozambique in the south and east. It has a population of about 10 million people, the majority of whom (>85%) reside in rural areas and are poor, deriving their livelihoods from small land holdings of between 1 to 2 ha per farm family of an average of five people (Chimunthu Banda, 2008).

Malawi is heavily dependent on natural resources, mainly soils, water, fisheries from inland lakes and fuel wood from forests. The biggest lake, Lake Malawi, drains freely into the Indian Ocean through the Shire River then the Zambezi (Chimunthu Banda 2008).



Figure 3, Maps of Malawi



2.2. Lower Shire River

The Shire River is the only outlet from Lake Malawi from which it meanders southwards for a distance of approximately 700 km to its confluence with the Zambezi River. About 95 % of the Shire River is situated in Malawi and the rest in Mozambique (Chimatiro, 2004). The Shire River is of great economic importance to Malawi. The Shire River generates more than 98 % of Malawi's electricity, supports abundant fisheries, and provides freshwater for irrigation in Malawi's plantations; as well as domestic and industrial uses. The Shire is generally divided into three sections, the upper, middle and lower Shire. The basins of the Shire River are important areas for the production of crops and for the preservation and conservation of forests and wildlife. Specifically, the floodplains, wetlands and forests of the

Lower Shire Valley are an important habitat for wildlife and for crop production (rice, cotton, beans, sorghum, millets and sugar cane) (Chimunthu Banda 2008).

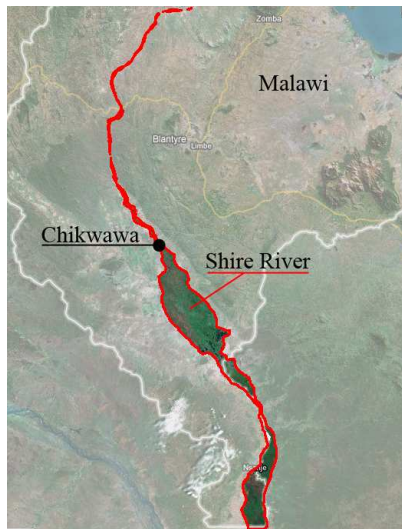


Figure 4, Lower Shire River, located down stream from Chikwawa



Figure 5, panorama photo of the floodplains of the Lower Shire River

The lower Shire River is located down stream from Chikwawa, figure 4. The Lower Shire River meanders frequently changing course through the Lower Shire floodplains, forming oxbow lakes, lagoons and islands. Appendix II holds detailed figure of the Lower Shire Valley. The Lower Shire falls in altitude from about 107 m.a.s.l. at Chikwawa to 61 m.a.s.l. at Nsanje, where the Shire enters Mozambique. The Lower Shire River has a length of approximately 250 km (Chimatiro 2004).

2.3. Climate of the Lower Shire Valley

Malawi has a sub-tropical climate, which is relatively dry and strongly seasonal. The climate of the Lower Shire Valley is characterized by two well-defined seasons; the hot-dry season from May to October, and the warm-wet season from November to April. Rains are generally low and with the onset dates varying significantly from year to year. Mean maximum monthly temperature in October and November is 27 °C, while mean minimum temperatures are in the range of 13 °C and 23 °C, in January and late October, respectively (Shire Valley Agricultural Development, 1975).

2.3.1. Precipitation

Annual average rainfall in Malawi varies from 725 mm to 2,500 mm ("Ministry of Lands and Natural Resources Malawi, Meteorological Services", n.d.). The Lower Shire Valley is located in a rain shadow resulting in a low annual precipitation ("Ramsar Sites Information Service", n.d.). Figure 6 shows the average monthly precipitation in the Lower Shire Valley. The precipitation is based on data received from the Department of Meteorological Services, Chikwawa Bomba 1971-2005 (Appendix III.5). The rain season lasts from December until March. From April until November the precipitation is low.

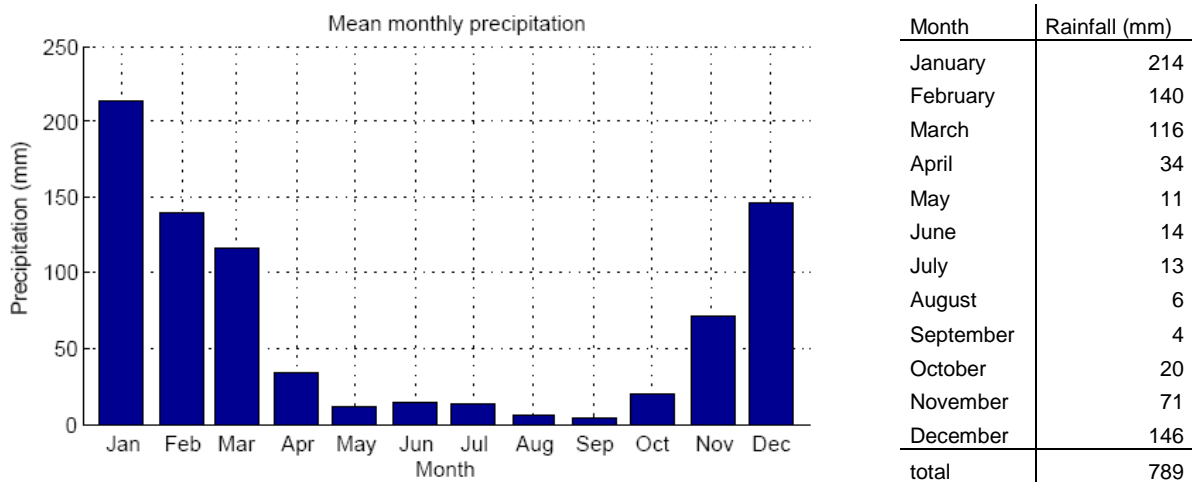


Figure 6, Mean monthly precipitation Lower Shire Valley

2.3.2. Air temperature

Temperatures in Malawi are greatly influenced by topography, being, for example, much warmer in the Lower Shire Valley than in the highlands. Over most of the country the annual range in temperature is about 12 °C. The lowest temperatures occur in June and July and the highest occur in October and November (“Ramsar Sites Information Service” ,n.d.).

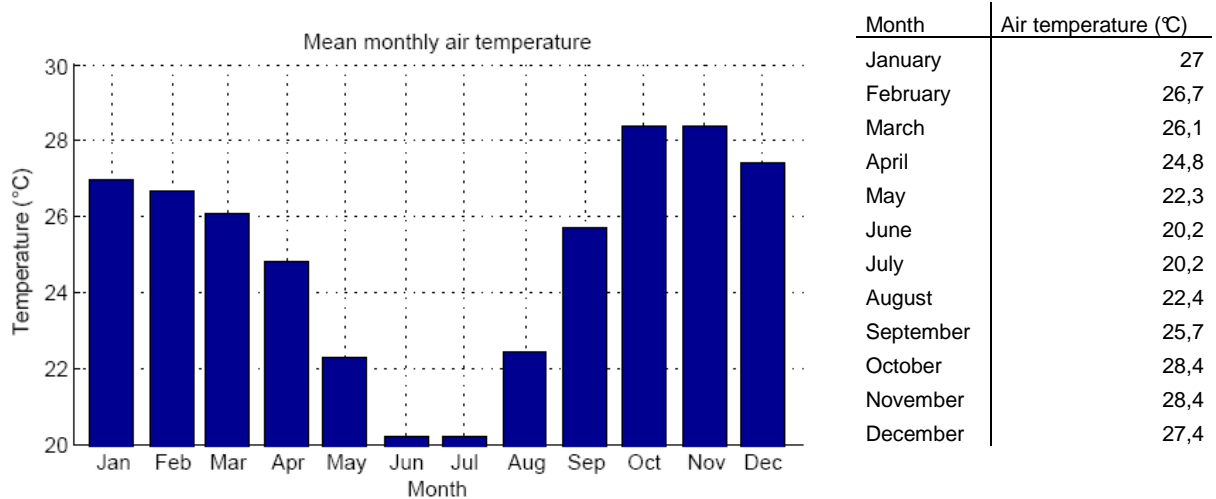


Figure 7, Mean monthly air temperature of the Lower Shire Valley, data based on measurements by Chimatiro (2004)

Data of the wind speed, cloud cover, water temperature and relative humidity of the Lower Shire Valley can be found in appendix II.

2.4. Hydrograph of the Lower Shire River

The three sections of the Shire River have unique characteristics that result in different flow and runoff patterns. The mean annual flow at Chikwawa is 511 m³/s (Chimatiro 2004). The annual hydrograph representing the flood regime in the Lower Shire Floodplain fits into four flood regime categories that correspond to the quarterly hydro-climatic seasons. These four

categories are: low in July to September, low-but-rising in October to December, peak in January to March, and falling or receding in April to June (Chimatiro 2004). Figure 8 is a typical hydrograph of the floodplain of the Lower Shire River which shows the different categories. In figure 3 the water level is relative to the river bottom. The Sodium content in the Shire River is estimated at 15 mg/L (Chimatiro 2004).

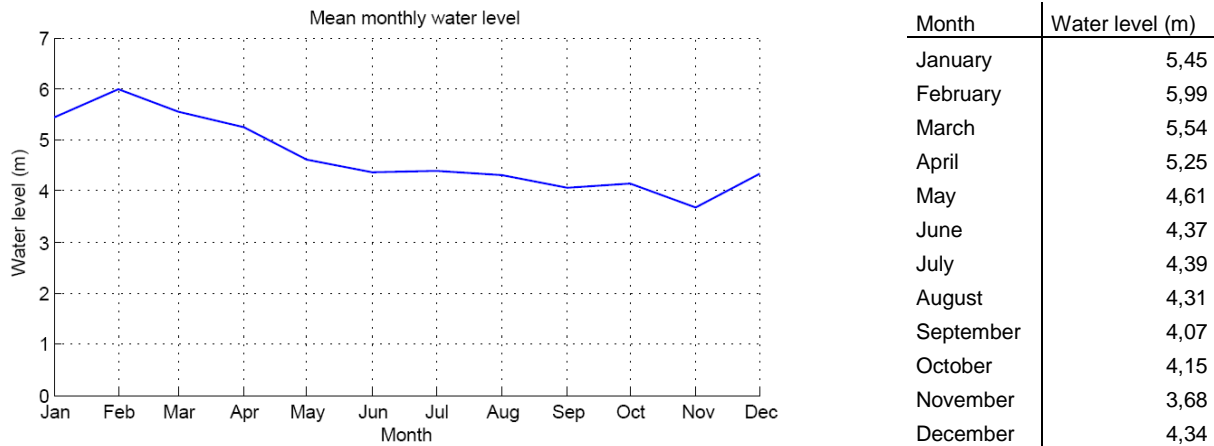


Figure 8, *Hydrograph of the floodplain of the Lower Shire River, at Chikwawa*

2.5. Floodplains Lower Shire River

The floodplains of the Lower Shire River are one of the seventeen major floodplains in Africa and directly benefit an estimated 1 million people in riparian communities in Malawi and Mozambique. It covers an estimated area of 1100 km² (Chimatiro, 2004). Seasonal changes in water flow make floodplain systems complex, dynamic and diverse habitats. This is mainly caused by the process of sediment deposition, which forms bars, levees, swales, ox-bow lakes, and backwaters (Lorenz 1997).

The parts of the floodplains of interest in this study are those which flood during the peak water level (January to March), water stays behind after the water level drops and dry out during the low water level period (April to December). Figure 9 is a situation sketch. The term floodplain in this report will from now on refer to the floodplains situated in figure 9.

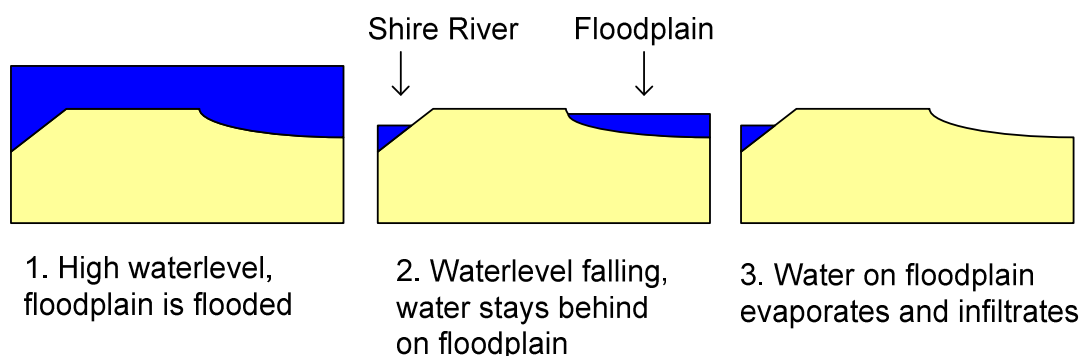


Figure 9, *Floodplain flooding and drying process*

2.5.1. Soil of the floodplains

Unfortunately no grain size distribution was received from Malawi to estimate the soil characteristics. Instead the average soil properties of clay and sandy clay are used, suggested by Per Aagaard. Table 1 holds the soil properties for clay and sandy clay (Dingman 2002).

Soil texture	porosity [-]	K_h^* [ms^{-1}]	ψ_{ae} [m]	b [-]
Sandy clay	0,426	$2,17 \cdot 10^{-6}$	0,153	10,4
Clay	0,482	$1,28 \cdot 10^{-6}$	0,405	11,4

Table 1, soil parameter values

In table one K_h^* is the saturated hydraulic conductivity, ψ_{ae} is the air entry tension and b is pore size distribution index.

2.5.2. Aquifers and salinity

Under the floodplains are two aquifers. A (1) shallow unconfined aquifer and a (2) deeper confined aquifer, figure 10. The shallow aquifer has a high content of salts and cannot be used for drinking water. The deeper confined aquifer is used for drinking water instead. The level of the ground water is approximately 0,5 m under the surface of the floodplain, estimation out of field measurement.

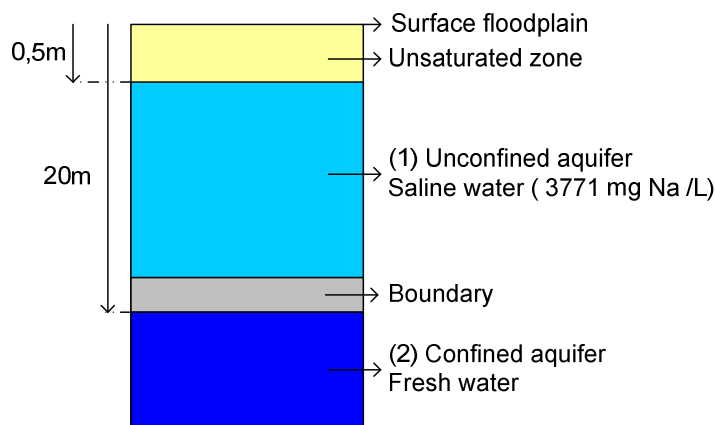


Figure 10, Profile of aquifers

According to the field measurements the sodium content of the unconfined aquifer is approximately 3771 mg/L, table 2. The confined aquifer is located at approximately 20 m deep. The aquifers are separated by a boundary. No information is available on the boundary.

S/N	Sample Description	Na (mg/L)
1	Site 1 water 20-40 cm	3967
2	Site 1 water 40-60 cm	3688
3	Site 2 water 40-60 cm	7278
4	Site 3 water 40-60 cm	150
Mean		3771

Table 2, water samples, field measurements by Maurice Monjerezi University of Malawi, Chemistry Department

3. Soil salinization processes

There are two possible soil salinization processes, soil salinization due to flooding and soil salinization due to capillary rise. Both processes are explained in this chapter.

3.1. Soil Salinization due to flooding

Figure 11 shows the soil salinization due to flooding. The process starts with the flooding of the floodplain. Water stays behind on the floodplain which infiltrates and evaporates. Soil salinization can only occur when the salinity of the water reaches a critical level (for NaCl approximately 310 g/l) (Gilman & Bear, 1994). Due to the evaporation the salinity of the flood water rises. This may lead to soil salinization.

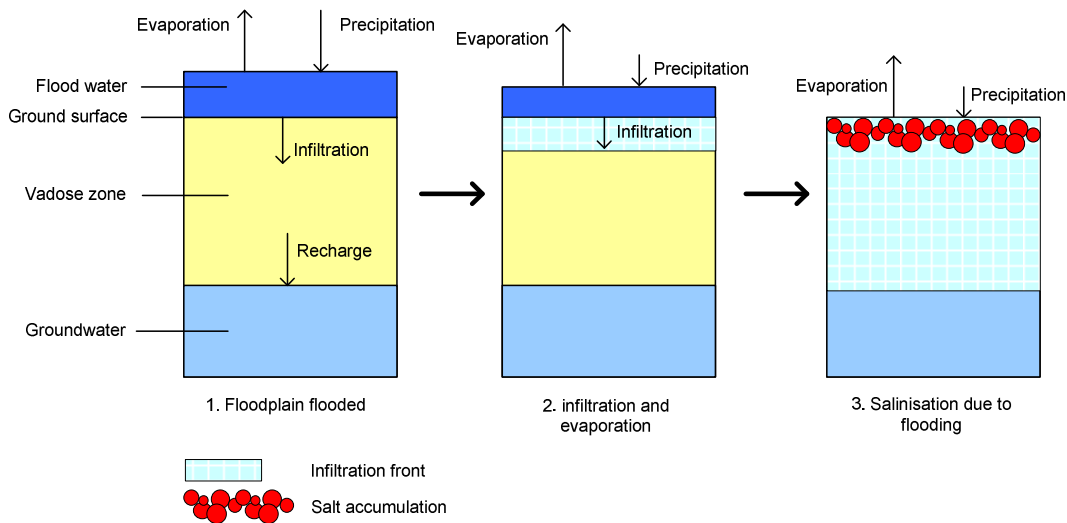


Figure 11, Soil salinization due to flooding

3.2. Soil Salinization due to capillary rise

Figure 12 shows the salinization due to capillary rise. When the water table is at a relative shallow depth and the area is evaporation dominated, water discharges from the groundwater in to the vadose zone and is directed upwards due to capillary rise. If groundwater is saline, this flow transports salts towards ground surface. Water evaporates from the upper soil layer, while salts remain in the soil and their concentration increases (Gilman & Bear, 1994).

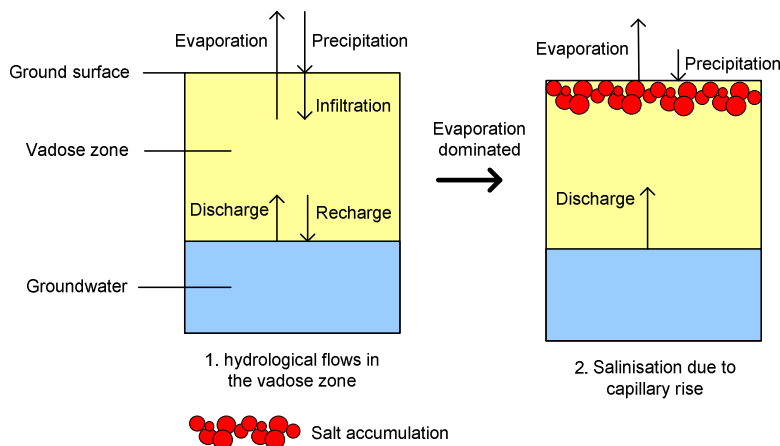


Figure 12, Soil salinization due to capillary rise

4. One dimensional soil water model

A model is a simplified representation of a real system, which is too complicated to formulate in complete detail. The fundamental goal of modeling within the scientific method is to understand how the real system works and to serve as a substitute for information that can be used to make predictions for real systems (Corwin, Letey & Carillo, 1999). To understand to the soil salinization the different processes that influence the soil salinization are simulated in a 1D numerical model. Numerical modeling plays an important role in studies of soil salinization, in particular in understanding the salinization processes and deriving strategies for salinization control (Xu & Shao, 2002).

4.1. Basics of the model

The two possible soil salinization processes have five main processes; evaporation, precipitation, infiltration, discharge and solute movement (figure 11 and figure 12). From these processes precipitation is described in paragraph 2.3.1. The other four processes are described in this paragraph.

4.1.1. Model assumptions

Because not all needed data is available the model is based on the following assumptions: (1) the groundwater level is constant in time, (2) the soil is homogeneous and isotropic, (3) the soil is bare, (4) the solute flux is zero at the soil surface, thus no chemicals are lost by evaporation, (5) the salinity of the groundwater is constant, (6) when evaporation exceeds precipitation the precipitation directly evaporates and does not infiltrate, (7) the groundwater flow is steady during Δt , (8) sodium chloride is representative for all salts, (9) there is enough chloride to form sodium chloride, (10) salt only accumulates in the top layer of the soil and (11) the groundwater flow is not affected by difference in salt concentration (osmotic potential, difference in water density). Some of the assumptions are explained further in this chapter.

4.1.2. Unsaturated water flow

Both infiltration and capillary rise are flows in the unsaturated zone and can be calculated with the Darcy's Law and the Richards Equation (Dingman, 2002):

$$\text{Darcy's Law} = V_z = K_z(\theta) \frac{\partial \psi(\theta)}{\partial z} - K_z(\theta)$$

$$V_z = \text{water flux in } z \text{ - direction [m/s]}$$

$$\theta = \text{water content} = \frac{V_w}{V_s} [-]$$

$$V_w = \text{water volume [m}^3\text{]}$$

$$V_s = \text{soil volume [m}^3\text{]}$$

$$K_z(\theta) = \text{hydraulic conductivity as a function of the water content [ms}^{-s}\text{]}$$

$$\psi(\theta) = \text{pressure head as a function of the water content [m]}$$

$$\text{Richards Equation} = \frac{\partial \theta}{\partial t} = \frac{\partial V_z}{\partial z} = -\frac{\partial K_h(\theta)}{\partial z} + \frac{\partial}{\partial z} \left[K_h(\theta) \cdot \frac{\partial \psi(\theta)}{\partial z} \right]$$

$$t = \text{time [s]}$$

To estimate the $K_h(\theta)$ and the $\psi(\theta)$ the empirical relation suggested by Campbell (1974) is used;

$$K_h(\theta) = K_h^* \left(\frac{\theta}{\phi} \right)^c$$

$$\psi(\theta) = |\psi_{ae}| \left(\frac{\phi}{\theta} \right)^b$$

K_h = hydraulic conductivity [ms^{-1}]

θ = water content [-]

ϕ = porosity [-]

ψ = pressure head [m]

ψ_{ae} = air - entry tension [m]

b = pore size distribution index [-]

$c = 2.b + 3$

Both the Richards Equation and Darcy's Law are non-linear because of the dependence of the hydraulic conductivity and the pressure head on the water content. To solve the flow equation numerical discretizations of Darcy's Law and the Richards equation are made. The discretizations can be found in appendix III

4.1.3. Solute movement

It has long been recognized (Slichter, 1905) that water and salt do not move at the same rate in soil. According to miscible displacement theory, salt moves in soil in response to two processes. The mass flow of water produces an imposed movement of salt, often called convective transport. Occurring simultaneously is the processes of diffusion, which is defined as salt movement in response to a concentration gradient (Shainberg & Shalhevet, 1984). The basic equation for steady-state solute movement under steady-state one-dimensional water flow in a homogeneous soil is (Addiscott & Wagenet, 1985)

$$VC_z = -[\theta.D_m(V_z) + D_p(\theta)] \frac{\partial C}{\partial z} + V_z.C$$

VC_z = steady state solute flux [g / s]

D_m = mechanical dispersion coefficient [$m^2 s^{-1}$]

D_p = diffusion coefficient [$m^2 s^{-1}$]

C = solute _ concentration [g / m]

z = depth [m]

$$\frac{\partial C}{\partial t} = - \frac{D \partial^2 C}{\partial z^2} + \frac{V_z \partial C}{\partial z}$$

t = time [s]

$D = [\theta.D_m(V_z) + D_p(\theta)]$ = apparent diffusion coefficient [$m^2 s^{-1}$]

To model the solute movement the apparent diffusion coefficient must be known. This coefficient is a function of the soil properties (grain size distribution ect), water content and water flux. A study to the apparent diffusion coefficient does not fall within the scope of this study. To simplify the solute movement, the effects of dispersion and diffusion are ignored which reduces the solute movement equation to $VC_z = V_z.C$ and $\frac{\partial C}{\partial t} = \frac{V_z \partial C}{\partial z}$. The discretization of the solute movement can be found in appendix III.

From observations it appears that most the salt that accumulates is sodium chloride (NaCl). No data is available on the chloride concentrations. Assumed is that there is enough chloride to form sodium chloride to precipitate. Sodium chloride precipitates when the concentration exceeds approximately 310 g/dm^3 (Gilman & Bear, 1994). This means that sodium precipitates at 122 g/dm^3 . The accumulation of sodium chloride will be representative for the salt accumulation

4.1.4. Evaporation

The model holds two types of evaporation; free-water evaporation and bare soil evaporation. The free water evaporation is used to estimate the evaporation from surface water (Dingman, 2002) and is discussed in paragraph 3.2.1. Bare soil evaporation is discussed in paragraph 3.2.2.

4.1.4.1. Free-water evaporation

Free-water evaporation is the evaporation that would occur from an open-water surface in the absence of advection and changes in heat storage and which thus depends only on regionally continuous meteorological or climate conditions (Dingman, 2002). The “standard” hydrological method for determination of free-water evaporation is the Penman equation (Dingman, 2002):

$$E = \frac{\Delta.(K + L) + \gamma.K_e.\rho_w.\lambda_v.v_a.e_a^*. (1 - W_a)}{\rho_w.\lambda_v.(\Delta + \gamma)}$$

$$\Delta = \frac{2508,3}{(T_a + 237,3)^2} \cdot \exp\left(\frac{17,3.T_a}{T_a + 237,3}\right)$$

$$T_a = \text{air temperature} [^{\circ}\text{C}]$$

$$K = \text{netto shortwave radiation} [MJm^{-2}day^{-1}]$$

$$L = \text{netto longwave radiation} [MJm^{-2}day^{-1}]$$

$$\gamma = \text{Bowen ratio} = 0.066 [kPaK^{-1}]$$

$$K_e = \text{water transport coefficient} [kPa^{-1}]$$

$$\lambda_v = \text{Latent heat vaporization} = 2,50 - 2,36 * 10^{-3} . T = 2,47 [MJkg^{-1}]$$

$$e_a^* = \text{saturated air vapor pressure} = 0,611 \cdot \exp\left(\frac{17,3.T_a}{T_a + 237,3}\right) [kPa]$$

$$W_a = \text{relative humidity} [-]$$

The Penman equation requires data of the net shortwave radiation, net longwave radiation, wind speed, air temperature and relative humidity. Data of the wind speed and the relative

humidity can be found in appendix II, the air temperature in paragraph 2.3.2. The net short wave radiation and net longwave radiation can be found in appendix IV. The vertical transport of water vapor (K_v) has an average value of $1,26 \cdot 10^{-3}$ (Dingman, 2002).

The total evaporation is the solution of the Penman equation. Figure 13 is a plot of the mean monthly free-water evaporation. The total evaporation, 2080 mm/year, matches with the estimations made by Chimatiro (2004), 2204 mm/year, and estimation made by Malawi Department of Water (1986), 1885 mm, pan evaporation at Kenyan.

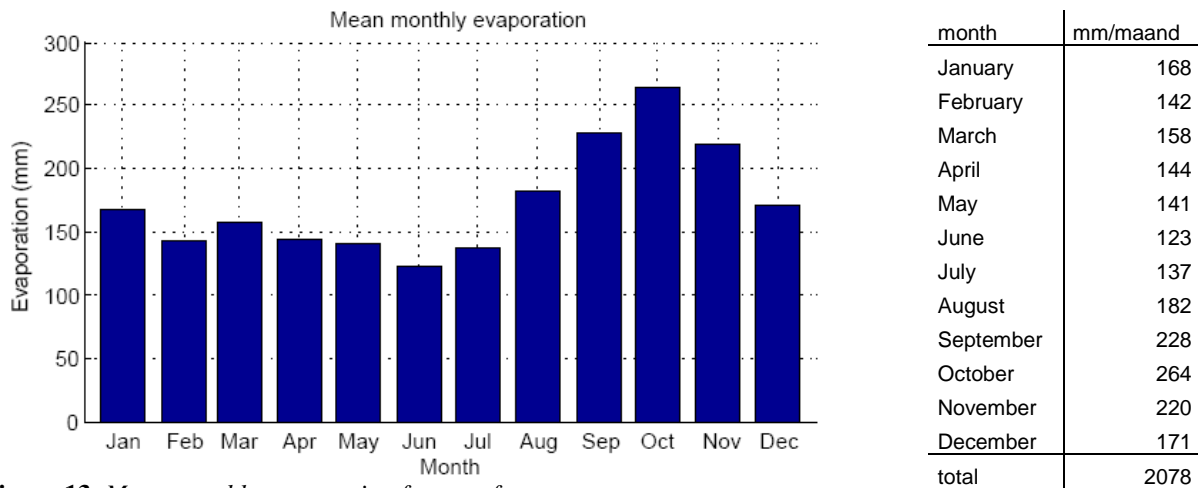


Figure 13, Mean monthly evaporation from surface water

4.1.4.2. Bare soil evaporation

Bare soil evaporation, also called exfiltration, generally occurs in two distinct stages (Dingman, 2002): (1) an atmosphere-controlled stage, in which the evaporation rate is largely determined by the surface energy balance and mass-transfer conditions, evaporation in this stage occurs at or near the rate of free-water evaporation and (2) a soil-controlled stage in which the evaporation is less than the free-water rate.

Stage one can be estimated best with the Penman Equation (Dingman 2002), evaporation occurs at the ground surface. When the demand of water through evaporation is higher than the maximum supply from the groundwater table the water content in the surface layer lowers. The water content lowers until the field capacity is reach. From this point stage two occurs. The evaporation in stage two is limited by the capillary rise from the groundwater table and the vapor flux through the soil. Gowing, Konukcu & Rose (2006) proposed a model where the bare soil evaporation in stage two is calculated through a balance between the water flux from the groundwater (capillary rise) and the flux of water vapor through the soil (diffusion).

Because the salt accumulation in the Shire Valley appears at the top part of the soil, the evaporation in stage two is assumed to be only limited by the water flux from the groundwater to the surface and evaporation only appears in the top part of the soil. This means that the evaporation in the simulation when stage two occurs will be lower than the evaporation proposed by Gowing et al. (2006).

4.2. Model

The model is programmed and run in Matlab, a numerical computing environment and programming language. This paragraph explains the different stages in the model and the configuration of the model.

4.2.1. Model stages

The model is based on the numerical discretizations presented in appendix III. The model contains six stages. Appendix VI contains the full Matlab script with the different stages in the script. Figure 14 is a chart with the different processes and input of each process. Stage 1 is the basic parameters. Here the basic numerical properties are defined like dt and dx . Second stage in the model is the soil and water properties. The model is simulated with two types of soil, sandy clay and clay. Both stage one and stage two can be seen as the input which can be adjusted to simulate different situations. Together with the climate data, evaporation and precipitation (3a), they form the total input of the model.

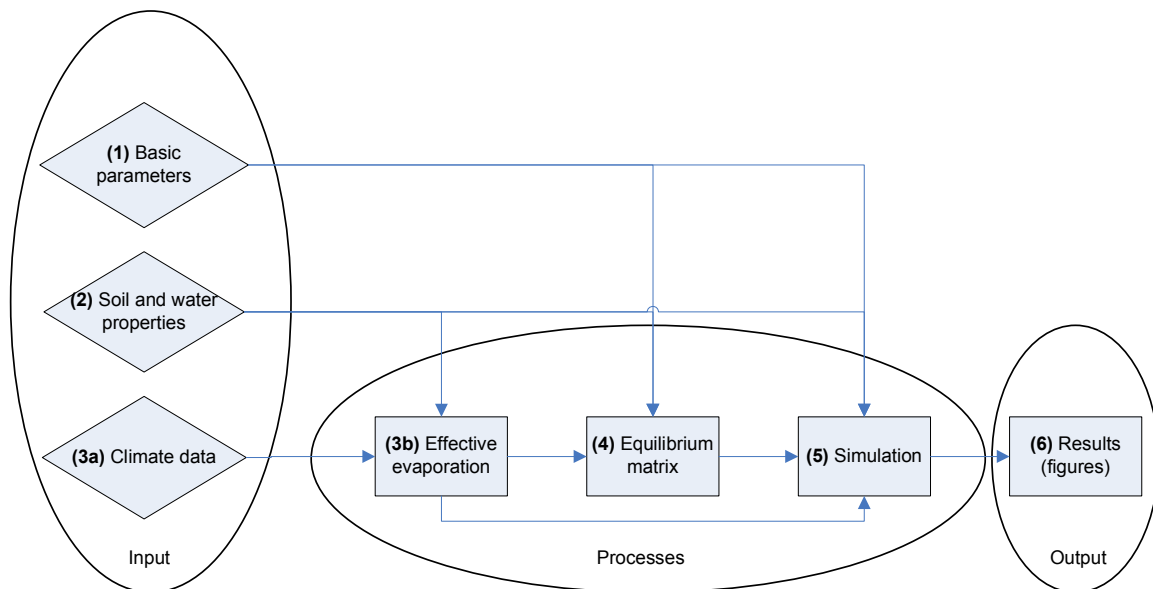


Figure 14, *Model input, processes and output*

In stage three-b two matrices are created which contain the evaporation and rainfall data with a time step of dt based on respectively mean monthly evaporation, paragraph 4.1.4, and mean monthly rainfall, paragraph 2.3.1. Both matrices are combined into one matrix, the effective evaporation. This matrix holds the evaporation minus the rainfall.

Stage four creates an equilibrium matrix which is used as initial condition for the actual simulation. The equilibrium simulation is run of 100 days where the effective evaporation is the average effective evaporation over the whole year. Because the outflow of water (effective evaporation) is constant in time the system will tend to equilibrium. This equilibrium is used as initial condition for the actual simulation.

Stage five is the actual simulation. The inputs are the parameters from stage one and two and the result of the equilibrium run. The simulation is a loop from $t=\text{start}$ until $t=\text{einde}$ with a delta t which can be adjusted in stage one. Within this loop several smaller loops are performed. The simulation loop starts with a back up of the water content in the top layer and

a back up from the water depth of the surface water (5.1). Phase two is the evaporation which is subtracted from the surface water. When the surface water is 0 the evaporation is subtracted from the top layer (5.2). Phase (5.3) is a restriction for the water content which cannot be lower than the minimum water content, the field capacity. In phase (5.4) the pressure head and the hydraulic conductivity as function of the water content are determined. Phase (5.6) is the calculation of the water flux between the layers. Phase (5.7) is a restriction, no water flux towards the ground water, the groundwater is already saturated. Phase (5.8) is also a restriction, no water flux towards the surface water from the top layer. In phase (5.9) the new water content is calculated at $t+dt$. The calculation of the new water content is done through a loop. This loop makes sure the water content at $t+dt$ is not higher than the saturation by restricting the water flux to a maximum. This restriction might have the result that now another layer becomes over saturated so the process is repeated the number of layers plus one times. Phase (5.10) sets the parameters of the groundwater and the high of the surface water at $t+dt$.

In phase (5.11) the salt movement is determined. The phase start with a matrix which holds the flow direction of the water fluxes (5.11.1). In phase (5.11.2) the new salt concentrations are calculated. Phase (5.11.3) how much salt accumulates into the top layer. Phase (5.11.4) creates a matrix which holds the amount of salt that accumulates per square meter. The matrix "layer" holds the water content, salt concentration and salt accumulation in time in the different layers. "layer(:, :, end)" is the final result.

In stage six two figures are created which hold the results of the simulation. Figure one is an overview of the water content, surface water, total water discharge from groundwater and effective evaporation in time. Figure two is the salt concentration and accumulation in time.

4.3. Model configuration

The input defines the actual out come. The model holds three groups of input; basic parameters, soil and water properties and climate data. The soil parameters used are shown in paragraph 2.5.1. The surface water level is set at 0.15 m and 0.4 m. Both values are simulated. Here 0.15 m represents a low water level and 0.4 m a high water level, estimation Per Aagaard. The climate data is shown in chapter two.

4.3.1. Delta t and delta x

The "basic properties" input holds the start and end date of the run, dt , dx and the length of the equilibrium run. The parameters dt and dx are very important. The smaller dt the more stable the model and the bigger dx the more stable the model. Preferred would be a very small dt and a small dx , this approaches the analytical solution best. Limiting factors are the simulating time and the stability. Different runs have shown that the minimum dt is 0,01 day. If dt would be smaller the simulation would crash due to a lack of memory. The value of dx is now limited by the stability of the model. Different runs have shown that a dx of 0,125 m is the smallest value where the model is still stable.

4.3.2. Maximum sodium concentration

The size of dx does not only influence the stability of the model, it also influences the amount of salt that accumulates. The maximum sodium concentration is 122 g/dm^3 . If dx would be small, for example 0.001 m, the sodium concentration in the top layer reacts stronger on evaporation and precipitation, rising and falling fast. With a dx of 0.125 m the sodium

concentration reacts slowly on evaporation and precipitation, rising and falling slow. Although the amount of sodium in the vadose zone would be almost equal when dx is 0.001 or 0.125, the salt accumulation would differ.

To compensate for this difference the maximum sodium concentration in the top layer is adjusted. If dx would be very small every evaporation flux would result in salt accumulation in the top layer. To create this situation the maximum sodium concentration should be a little higher than the sodium concentration in the groundwater. This way a little increase of the sodium concentration leads to salt accumulation. Adjusting the maximum sodium concentration can also be a way to compensate for diffusion and dispersion which are left out of the model. If the maximum sodium concentration is for example 20 gram/dm³ and dx is 0,125 m than salt accumulation would only occur when the top layer is saturated. This means that the top layer contains for 0,125 m a sodium concentration of 20 gram/dm³. No data is available to calibrate the maximum sodium concentration to the actual salt accumulation. The maximum sodium concentration is set on 30 gram/dm³. This is a rough estimation.

4.3.3. Duration of simulation

The start of the simulation is 1 April, the date that the floods are over, see paragraph 2.5. The end of the simulation is 31 December, the date that the floods starts, see paragraph 2.5. The length of the equilibrium run is set to 100 days. Simulating the equilibrium more than 100 days does not change the result significant.

5. Results

Four scenarios are simulated. Two scenarios with sandy clay and two scenarios with clay. Both sandy clay and clay are simulated with a surface water level of 0.15 m and 0.4 m.

5.1. Run 1: sandy clay and 0,4 m surface water

Run 1 is a simulation with sandy clay as soil and a surface water level of 0,4 m. Figure 15 is a representation of the water flow in the vadose zone in time. At first water infiltrates from the surface into the ground. Result is that the water content in the top layer quickly rises until saturated. Around day 180 all the surface water has evaporated and water starts to evaporate from the top layer. After approximately 10 days the systems reaches equilibrium where the discharge is equal to the effective evaporation. When the effective evaporation changes the equilibrium shifts to a new equilibrium. In December the effective evaporation is negative which results in an increase of the water content.

Figure 16 is a graph of the sodium concentration and salt accumulation in time. In the sodium concentration graph the dotted line is the sodium in the surface water and the full line is the sodium concentration in the top layer. The sodium concentration in the surface water rises exponential and tends to zero around day 180, when all the water has evaporated and the salt in the surface water accumulates. Now water starts to evaporate from the top layer and the sodium concentration rises in the top layer. The concentration rises until the maximum sodium concentration in water and starts to precipitate when more water evaporates resulting in salt accumulation. The total salt accumulation due to flooding is 0,013 kg/m² and the total salt accumulation due to capillary rise is 5,003 kg/m², making a total salt accumulation of 5,0 kg/m².

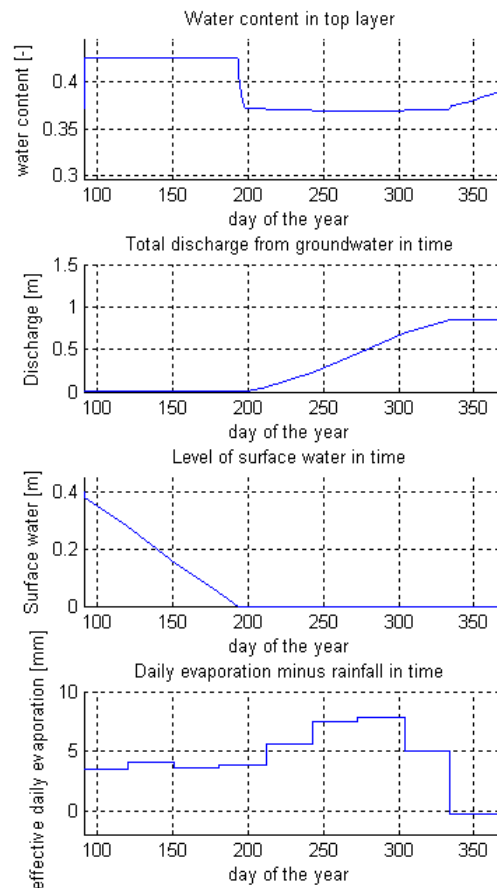


Figure 15, water flow in the unsaturated zone, run 1

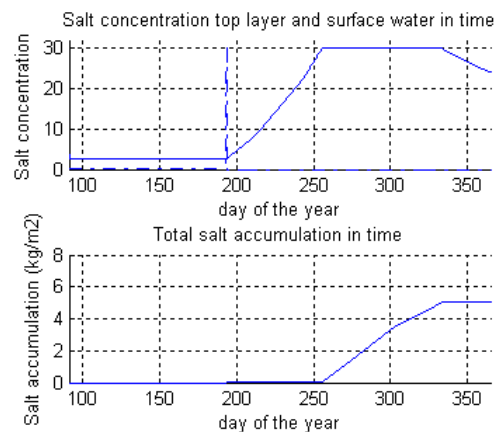


Figure 16, sodium concentration and salt accumulation, run 1

5.2. Run 2: sandy clay and 0,15 m surface water

Run 2 is a simulation with sandy clay as soil and a surface water level of 0,15 m. Figure 17 is a representation of the water flow in the vadose zone in time. Difference with run 1 is the time it takes for the surface water to evaporate. This results in a higher total water discharge from the groundwater.

Figure 18 is a graph of the sodium concentration and salt accumulation in time. In the sodium concentration graph the dotted line is the sodium in the surface water and the full line is the sodium concentration in the top layer. Because the surface water has evaporated more quickly the sodium concentration reaches saturation faster than in run 1. More water is discharged from the groundwater resulting in a higher salt accumulation due to capillary rise, $7,399 \text{ kg/m}^2$. The salt accumulation due to flooding is lower, $0,003 \text{ kg/m}^2$. The total salt accumulation is $7,4 \text{ kg/m}^2$.

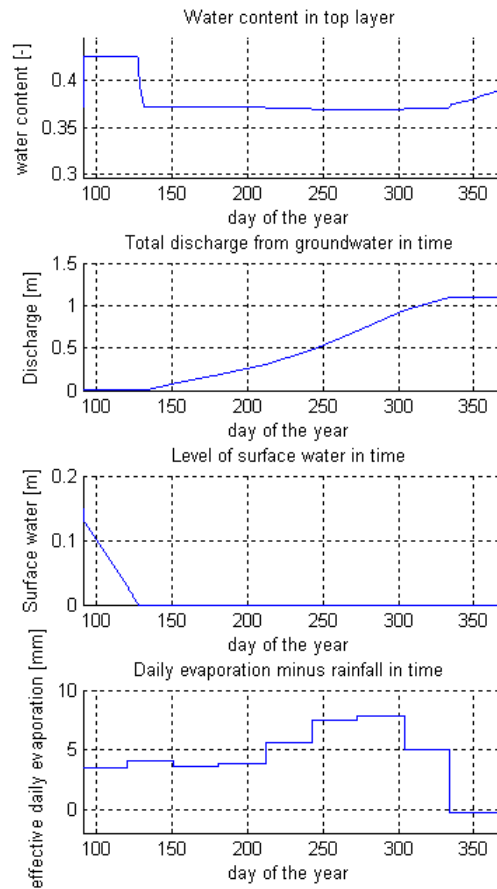


Figure 17, water flow in the unsaturated zone, run 2

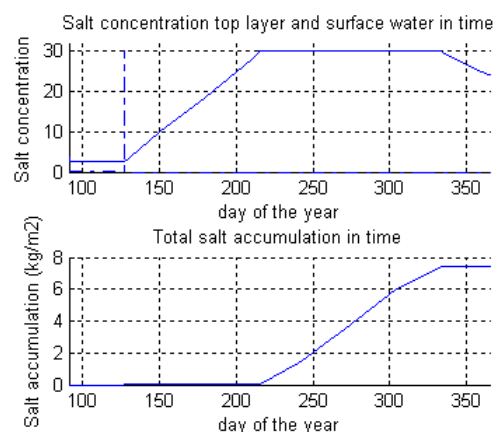


Figure 18, sodium concentration and salt accumulation, run 2

5.3. Run 3 and 4

Table 3 holds the results of the four simulation runs. The results of run 3 and 4 in form of a plot can be found in appendix V. From table 3 can be concluded that the influence of soil salinization due to flooding can be neglected compared with the soil salinization due to capillary rise. The difference in total salt accumulation between the different soil types is small. The amount of salt accumulation due to capillary rise is very high. To validate the results data is needed on soil salinization.

Soil	Surface water [m]	Salt due to flooding [kg/m ²]	Salt due to capillary rise [kg/m ²]	Total salt accumulation [kg/m ²]
Sandy clay	0,4	0,013	5,003	5,0
Sandy clay	0,15	0,003	7,399	7,4
Clay	0,4	0,014	4,340	4,4
Clay	0,15	0,004	6,736	6,7

Table 3, results of simulation 1, 2, 3 and 4.

5.4. Influence of groundwater level

The influence of the groundwater is studied by performing seven simulations. In these simulations there is no surface water and the soil is clay. Figure 19 holds a graph with the total salt accumulation as a function of the groundwater level.

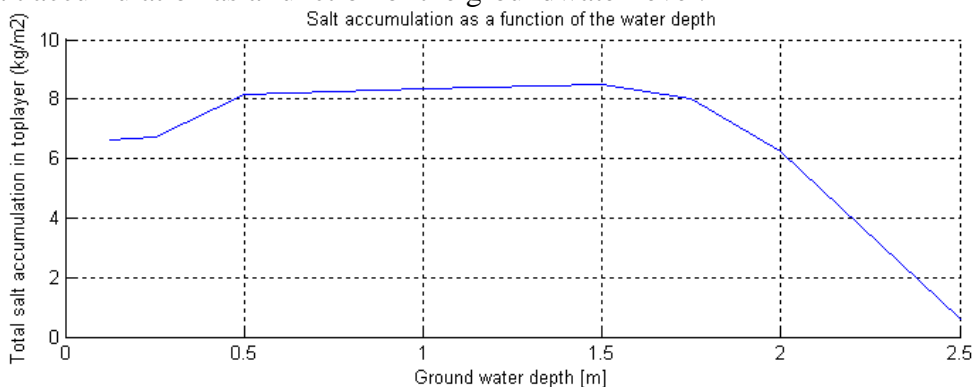


Figure 19, total salt accumulation as a function of the groundwater depth

The graph is not what is expected. According to the simulation the salt accumulation reaches a maximum when the water depth is around 1,5 m. More logical would be, the lower the water depth the higher the higher salt accumulation. According to the simulation the salt accumulation tends to zero when the groundwater depth exceeds 2,5 m. From this point not enough water can be discharged from the groundwater to the soil surface to cause soil salinization at the soil surface.

5.5. Influence of effective evaporation

Also the influence of the effective evaporation is studied. The effective evaporation is a representation of the climate in the Shire Valley. Figure 20 is a graph between the added daily evaporation and the total salt accumulation simulated in the model. In this run the set up of run 2 is used, only the effective evaporation is varied. If the added effective evaporation is for

example 6 mm, the n the daily effective evaporation is the daily effective evaporation on a certain day, say 4 mm for a day in April, plus 6 mm is a total of 10 mm a day.

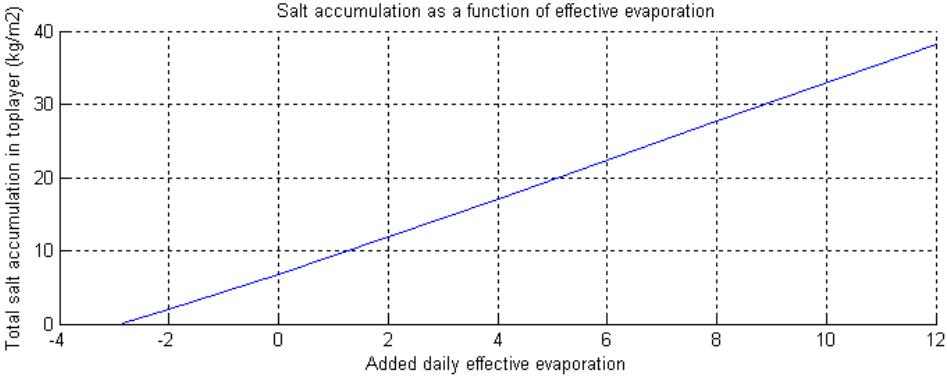


Figure 20, total salt accumulation as a function of the effective evaporation

The graph in figure is a straight line, which is not expected. At some point the daily effective evaporation should become so high that the groundwater cannot discharge enough water to the top layer. This means that no more water can be discharged to the top layer also no more salt can be transported to the top layer and the total salt accumulation should tend to a maximum. This does not occur, even if the yearly evaporation is more than 4m a year, the water discharged from the groundwater until the top layer is 4 m a year. This means that the soil controlled stage of the evaporation does not occur in the model (see paragraph 4.1.4.2 for soil controlled evaporation).

6. Discussion

From paragraph 5.4 and 5.5 it can be concluded that the model holds errors. There are many possible reasons for the errors. These could be: errors in the empirical equations of the hydraulic conductivity and the pressure head, errors in the climate data, errors in groundwater data, errors in the basics of the model, errors in the evaporation, errors in the solute movement, errors in the groundwater and errors due to instability.

6.1. Errors types

Using the empirical relation of the hydraulic conductivity and the pressure head could cause major errors in the unsaturated water flow when reaching the limits of the water content (minimum and maximum). The equations are strong exponential equations. When the water content tends to its minimum the values of the pressure head become very high and the hydraulic conductivity very low. When reaching these extreme values errors might occur. This could cause the extreme water discharge shown in paragraph 5.3.5.

The climate data used was not very accurate but within the boundaries of valid. The error caused by an error in the climate data cannot cause the errors within the model. Also the evaporation rate matches with values gathered from the literature as do the values for the precipitation.

The groundwater data is collected in the field of the floodplains. All the field measurements point to a very high salinity in the groundwater and a very low groundwater level. It is very likely these field measurements are correct. Also the field measurements cannot explain the errors in the model.

Errors in the basics of the model could cause the problems seen in paragraph 5.3.4 and paragraph 5.3.5. The discretizations used are most likely correct and the script built in Matlab is most likely also correctly written. Validations of the basics of the model can be done through an expert or through calibration and validation.

Evaporation is a function of a lot of variables. One of these variables is the water tension of the water which evaporates. This tension is not included in the Penman equations. This might cause an error in the amount of water that evaporates. This possible error needs more research on evaporation.

The solute movement is simplified to an advective solute flux. Diffusion and dispersion are neglected. This could cause an error in the amount of salt that actually accumulates. The maximum sodium concentration used in the model, 30 gr/L, is also a very rough estimation which is not validated. Also two processes which influence the water flow and the solute flow have been neglected. This is the osmotic potential and the density difference of water due to salt concentration difference. Although the solute movement is strongly simplified they could not cause the problem seen in paragraph 5.4 and paragraph 5.5.

In the model the groundwater level is at a constant level. The level would normally vary due to the discharge of water from the groundwater level and recharge from groundwater flows in the x and y direction. The variation in the groundwater can influence and limit the amount of water that can be discharged from the groundwater and so limit the amount of salinization.

Instability can cause a variety of problems. It could cause the problems seen in paragraph 5.4 and paragraph 5.5. The graphs from the simulation 1, 2, 3 and 4 show no instability in the model. A way to make the model more accurate is to decrease dt. To do this the script needs to be written in a different code which calculates the loops faster. There are some options; one of them is a so called “C function” which uses “Mex files”. This would increase the time to run the model, and make it possible to decrease dt to 0,001 day or lower. This way dx can also be lowered and the numerical solution approaches the analytical solution better.

7. Conclusion

As stated, the model holds errors. Also because the lack of data the model could not be calibrated nor validated. This also means that the exact amount of salt accumulation calculated by the model is unreliable. More important is if the goal of the research is achieved.

Goal of the research is to determine if the soil salinization on the Floodplains of the Lower Shire River is caused by flooding or by capillary action, by performing a literature study and setting up a 1D soil water model.

According to the model, soil salinization due to capillary rise causes more than 500 times more salt accumulation than soil salinization due to flooding. Although the model holds errors, the difference is large enough to conclude that the soil salinization is caused by capillary rise and not by flooding. The soil salinization processes occurs mainly during the hot-dry season. During the warm wet season there is too much precipitation and the flooding stops the discharge of groundwater to surface of the soil. The exact amount of salt accumulation due to capillary rise cannot be concluded from the model because of the errors.

The list of possible errors is long and it makes the model unreliable. But although the model holds a lot of possible errors which need to be studied, it is very transparent. Most models only use input and output and the actual calculations are unknown. To make better estimations of the soil salinization more data is needed on the soil and the soil parameters (pressure head and hydraulic conductivity) which strongly influence the flow of water in the vadose zone. Also more data is needed about the flooding process, the apparent diffusion coefficient, and the groundwater level in time. With more research the performance of the model could be increased greatly, and eventually it can be used to make real estimations of soil salinization.

8. References

- Addiscott, T.M. & Wagenet, J. (1985) Concepts of solute leaching in soils: a review of modelling approaches. *Journal of soil science*, 36, 411-424.
- Campbell, G.S. (1974). A simple method for determining unsaturated conductivity from moisture retention data. *Soil science*, 117: 311-314.
- Chimatiro, S.K. (2004) *The Biophysical dynamics of the Lower Shire River floodplain fisheries in Malawi*. Retrieved September 10, 2008, from Rhodes University, Web site: http://eprints.ru.ac.za/177/01/Chimatiro_PhD.pdf
- Chimunthu Banda, H.F. (2008). *Malawi's National Adaptation Programmes of Action (NAPA)*. Retrieved July 29, 2008, from Government of Malawi, Ministry of Mines, Natural Resources and Environment Environmental Affairs Department, Web site: <http://www.sarpn.org.za/documents/d0003013/index.php>
- Corwin, D.L., Letey, J. Jr., & Carillo, M.L.K., (1999). Modeling non-point source pollutants in the vadose zone: Back to basics. In: D.L. Corwin, K. Loague & T.R. Elsworth (Eds) *Assessment of Non-Point Source Pollution in the Vadose Zone, Geophysical Monograph 108, American Geophysical Union, Washington, DC*.
- Department of Environmental Affairs, Malawi (2002) *State of the Environment Report 2002*. Retrieved September 26, 2008, Web site: <http://www.sdn.org.mw/enviro/chilwa/ministry/stateenv2002/index.html>
- Diabaté, L., Blanc, Ph., Wald, L. (2004). Solar radiation climate in Africa. *Solar Energy*, 77, 733-744.
- Dingman, S.L. (2002) *Physical hydrology- 2nd edition*. Upper Saddle River, NJ: Prentice-Hall
- Gilman, A., Bear, J. (1994). The influence of free convection on soil salinization in arid regions. *Transport in porous Media*, 23, 275-301.
- Gowing, J.W., Konukcu, F., Rose, D.A. (2006). Evaporative flux from a shallow watertable: The influence of a vapour-liquid phase transition. *Journal of hydrology*, 321, 77-89.
- Hillel, D., (1980). *Fundamentals of Soil Physics*. Academic, New York, pp. 233-244
- Lorenz, C.M. (1997) Concept in river ecology: implications for indicator development. *Regulated Rivers: Research and Management*. 13: 501-516.
- Malawi Industrial Research and Technology Development Centre (2000). *Technology Strategy for Sustainable Livelihood, A Paper on Enterprise Development*.
- Ministry of Lands and Natural Resources Malawi, Department of Meteorological Services (n.d.). Retrieved 5 October 2008, from <http://www.metmalawi.com/climate/climate.php>

- Mkanda, F.X. (1999) Drought as an analogue climate change scenario for prediction of potential impacts on Malawi's wildlife habitats. *Climate research*, 12: 215–222.
- Ramsar Sites Information Service (n.d.). Retrieved 24 September 2008, from <http://ramsar.wetlands.org/Portals/15/MALAWI.pdf>
- Salama, R.B., Otto, C.J., Fitzpatrick, R.W. (1990) Contributions of groundwater conditions to soil and water salinization. *Hydrogeology Journal*, 7:46–64.
- Scofield, R., Thomas, D. S. G. & Kirkby, M. J. (2001). Causal processes of soil salinization in Tunisia, Spain and Hungary. *Land degradation & development*, 12, 163-181.
- Shainberg, I. & Shalhevet, J. (1984). *Soil salinity under irrigation*. Springer-Verlag, Berlin Heidelberg New York Tokyo.
- Shire Valley Agricultural Development, Project (1975) *An atlas of the Lower Shire Valley, Malawi*. Blantyre, Malawi. Department of Surveys.
- Slichter, C.S. (1905). Field measurements of the rate of movement underground waters. *USGS Waters Supply Irrigation*, 140, Washington DC.
- The U. S. Department of Agriculture (1998) *Soil Quality Resource Concerns: Salinization*, retrieved from <http://soils.usda.gov> .
- U.S. Department of the Interior, U.S. Geological Survey (2006) *Unsaturated Zone*. Retrieved July 26, 2008, Web site http://toxics.usgs.gov/definitions/unsaturated_zone.html
- Vogt, R.D. (2008) *Folk page Rolf D. Vogt*. Retrieved July 30, 2008, from University of Oslo, Web site: <http://folk.uio.no/rvogt/>
- Wang, Y., Xiao, D., Li, Y. & Li, X. (2007) Soil salinity evolution and its relationship with dynamics of groundwater in the oasis of inland river basins. *Environ Monit Assess*, 140: 291–302.
- Xu, P., Shao, Y. (2002). A salt-transport model within a land-surface scheme for studies of salinization in irrigated areas. *Environmental Modelling & Software*, 17, 39-49.
- Yaalon, D. H. (1967). Salinization and salinity. *Journal of chemical Education*, 44, 591-593

Appendices

Appendix I, Map of the Lower Shire Valley

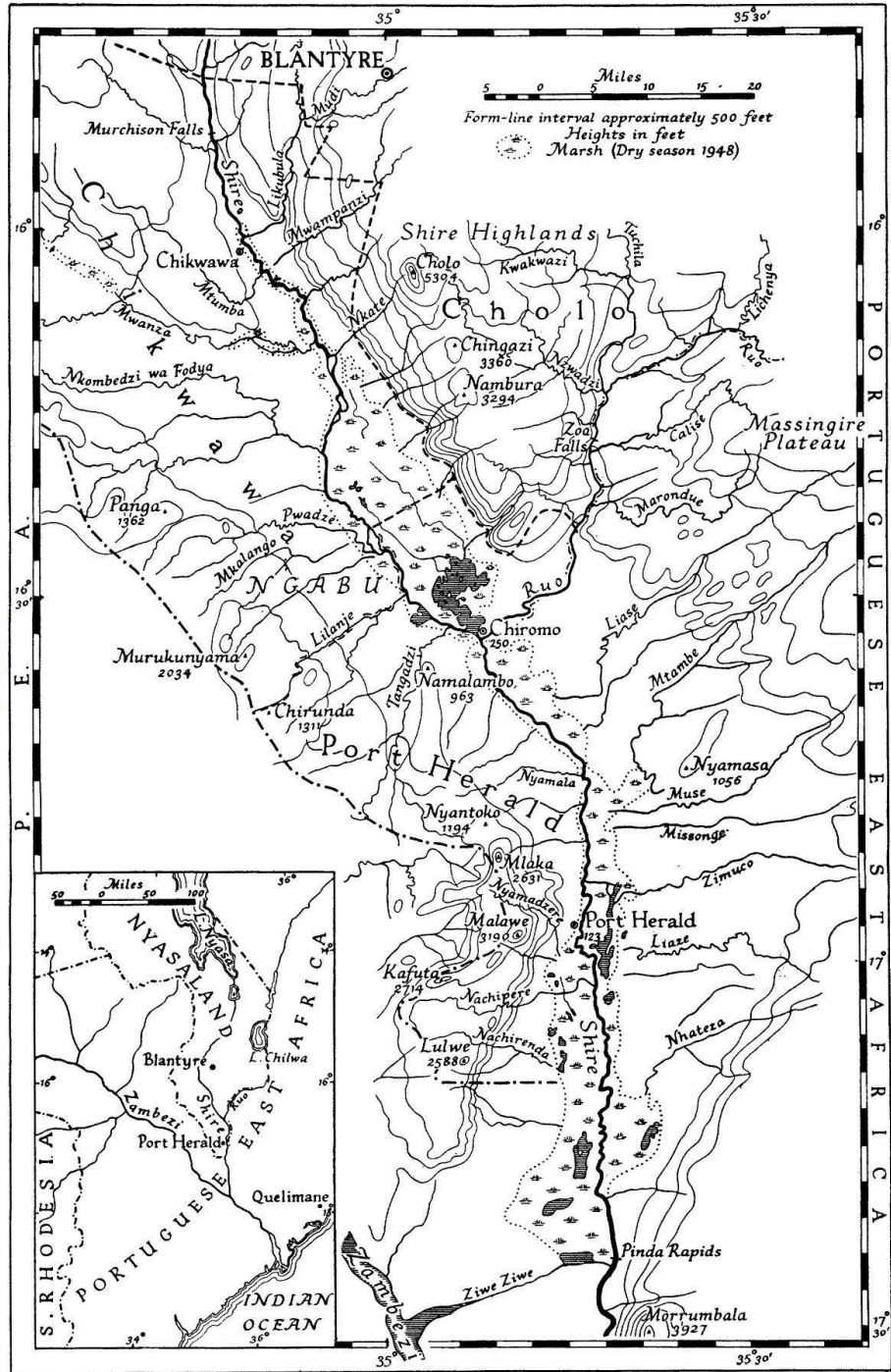
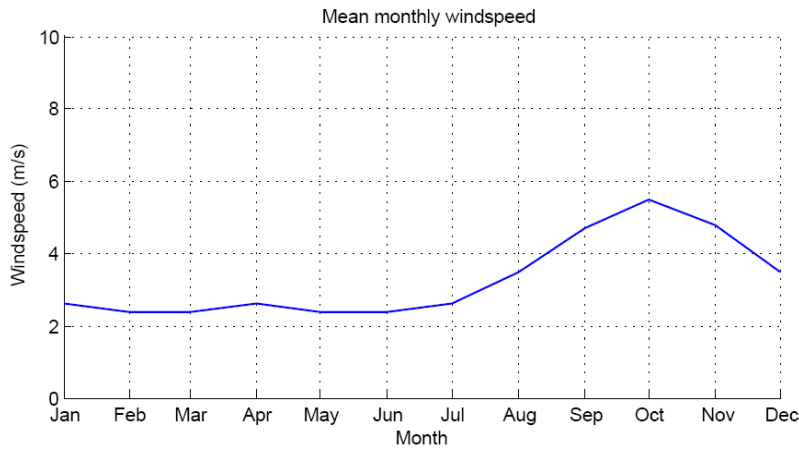


Figure 21, The Lower Shire Valley of Nyasaland

Appendix II, Climate data

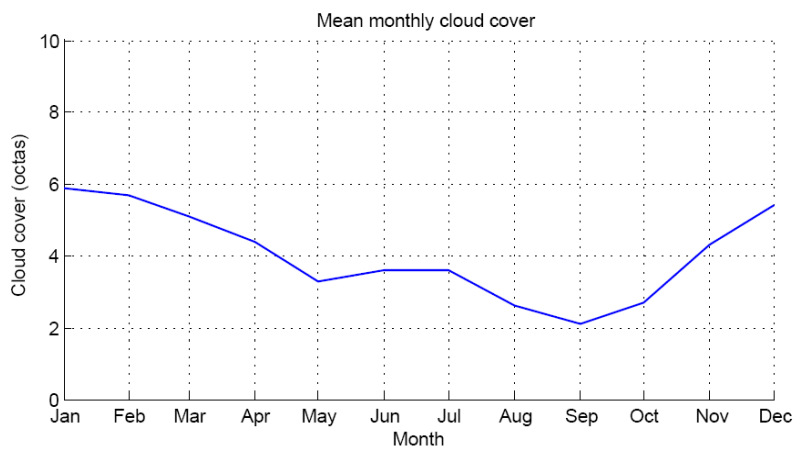
II.1. Windspeed



Month	Wind (m/s)
January	2.6
February	2.4
March	2.4
April	2.6
May	2.4
June	2.4
July	2.6
August	3.5
September	4.7
October	5.5
November	4.8
December	3.5

Figure 22, Mean monthly wind speed, data based on measurements by Chimatiro (2004)

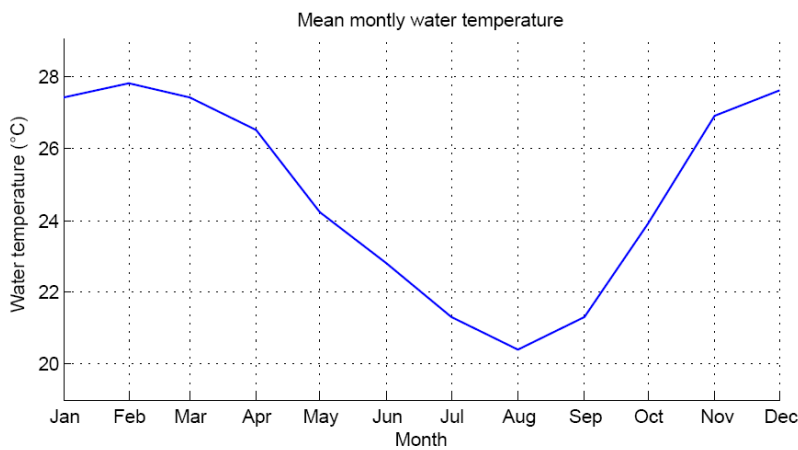
II.2. Cloud cover



Month	Clouds (octas)
January	5.9
February	5.7
March	5.1
April	4.4
May	3.3
June	3.6
July	3.6
August	2.6
September	2.1
October	2.7
November	4.3
December	5.4

Figure 23, Mean monthly cloud cover, data based on measurements Chimatiro (2004)

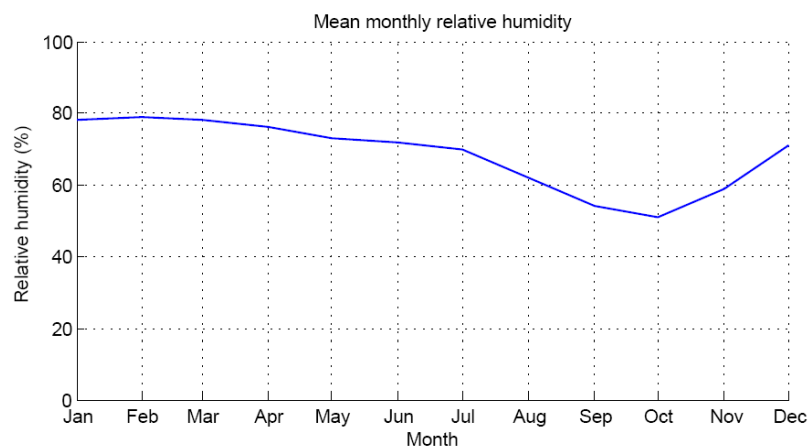
II.3. Water temperature



Month	Water temperature (°C)
January	27.4
February	27.8
March	27.4
April	26.5
May	24.2
June	22.8
July	21.3
August	20.4
September	21.3
October	23.9
November	26.9
December	27.6

Figure 24, Mean monthly water temperature, data based on measurements Chimatiro (2004)

II.4. Relative humidity



Month	Relative Humidity (%)
January	74
February	77
March	76
April	73
May	71
June	71
July	65
August	58
September	54
October	53
November	56
December	70

Figure 25, Mean monthly relative humidity, data received from the Department of Meteorological Services, Ngabu 1972-2006

NGABU MEAN MONTHLY RELATIVE HUMIDITY

SEASON	JAN	FEB	MAR	APR	MAY	JUN	JUL	AUG	SEP	OCT	NOV	DEC
1972	82	73	82	73	67	79	69	59	52	49	58	68
1973	69	71	79	72	65	70	66	60	54	52	48	72
1974	74	83	78	77	77	67	67	56	54	62	52	64
1975	80	81	76	77	69	72	63	58	60	58	61	65
1976	76	70	62	69								
1977	69	82	82	77	74	74	67	59	54	49		77
1978	82	80	80	75	71	66	63	58	50	51	59	90
1979	80	81	78	80	74	72	61	54	53	59	62	67
1980	75	71	65	69	63	66	55	54	53	50	47	63
1981	70	79	81	71	79	73	76	66	53		61	68
1982	71	84	79	77	75	75	66	57	56	54	61	75
1987	75	71	65	69	63	66	55	54	53	50	47	63
1988	70	79	81	71	79	73	76	66	53		61	68
1989	71	84	79	77	75	75	66	57	56	54	61	75
2005				61	62	66	65	53	52	49	48	65
2006	70	66	73	65								
Total	74	77	76	73	71	71	65	58	54	53	56	70

II.5. Rainfall

CHIKWAWA BOMA : MONTHLY AND SEASONAL RAINFALL TOTALS (mm)

SEASON	JUL	AUG	SEPT	OCT	NOV	DEC	JAN	FEB	MARCH	APRIL	MAY	JUNE	TOTAL
1971/72	4.3	0.0	0.0	0.8	162.8	126.2	182.1	122.7	88.6	10.2	4.8	23.9	726.4
1972/73	8.4	8.4	0.0	0.0	141.2	50.5	423.4	42.7	70.4	71.4	7.9	16.8	841.1
1973/74	24.1	8.1	0.0	3.8	85.6	135.6	150.6	137.9	129.3	46.2	15.0	28.7	764.9
1974/75	29.7	7.4	9.4	0.0	98.8	110.5	154.9	101.6	44.7	13.0	14.2	20.1	604.3
1975/76	1.3	3.8	0.0	116.1	114.3	196.1	30.2	174.2	206.7	42.2	50.3	38.7	973.9
1976/77	14.0	0.3	0.0	20.1	9.1	349.5	103.4	74.4	153.2	8.9	0.3	7.4	740.6
1977/78	2.0	3.6	11.4	0.0	37.3	193.0	201.9	74.7	220.7	51.6	5.3	17.5	819.0
1978/79	21.1	0.0	0.0	32.3	73.9	273.8	189.5	130.3	229.4	5.8	8.4	41.1	1005.6
1979/80	38.9	0.3	3.6	22.4	80.5	187.7	92.5	65.0	251.0	13.6	23.1	21.8	800.4
1980/81	0.0	8.8	12.1	3.2	17.5	209.5	212.1	205.8	49.4	33.7	12.4	6.2	770.7
1981/82	15.7	0.0	8.3	8.9	14.3	113.4	187.4	201.4	19.5	67.1	27.6	6.8	670.4
1982/83	54.2	52.1	8.6	89.4	18.0	93.0	83.9	134.2	72.0	0.0	12.0	0.0	617.4
1983/84	18.8	8.8	0.0	18.1	49.3	221.3	59.0	132.9	61.6	34.6	7.2	6.5	618.1
1984/85	0.0	5.6	0.0	21.0	54.5	128.5	156.4	142.5	199.7	132.1	9.0	9.2	858.5
1985/86	7.7	13.9	0.8	38.8	85.7	166.1	354.1	132.3	56.3	103.8	1.8	31.7	993.0
1986/87	39.0	0.0	5.8	92.8	72.8	154.3	195.5	11.1	49.1	28.5	10.3	23.0	682.2
1987/88	0.0	0.0	0.0	34.6	129.4	137.2	168.4	138.4	124.2	8.1	32.2	0.0	772.5
1988/89	26.6	3.1	0.0	36.3	27.5	90.6	227.9	205.7	427.7	39.6	0.0	38.5	1123.5
1989/90	3.3	8.0	7.1	9.6	62.4	98.2	202.4	94.7	63.5	19.6	31.2	38.5	638.5
1990/91	0.0	0.0	0.0	0.0	50.2	58.3	240.7	58.7	156.3	27.0	0.0	0.0	591.2
1991/92	0.0	0.0	0.0	0.0	62.0	20.1	124.3	7.4	206.3	0.0	10.3	0.0	430.4
1992/93	0.0	0.0	0.0	29.5	141.8	150.9	417.4	149.2	16.7	0.0	0.0	0.0	905.5
1993/94	4.6	16.0	0.0	12.5	97.4	49.1	172.0	91.2	63.6	0.0	0.0	0.0	506.4
1994/95	5.0	5.0	0.0	16.9	23.8	70.0	232.7	38.8	0.0	26.8	0.0	0.0	419.0
1995/96	0.0	0.0	0.0	0.0	65.0	346.1	224.0	274.8	167.1	66.1	17.2	45.2	1205.5
1996/97	0.0	0.0	0.0	16.0	93.8	293.3	357.2	592.6	59.6	27.6	0.0	0.0	1440.1
1997/98	0.0	0.0	0.0	17.0	54.2	97.4	279.6	144.7	69.8	13.6	1.8	0.0	678.1
1998/99	0.0	12.6	0.0	0.0	72.2	220.0	336.5	199.3	107.6	84.3	3.4	8.9	1044.8
1999/00	18.5	0.3	61.1	8.4	89.2	80.0	246.0	166.8	70.8	27.1	16.0	6.9	791.1
2000/01	23.4	4.3	0.0	5.5	165.4	70.5	279.0	270.3	164.1	52.4	0.0	0.0	1034.9
2001/02	0.0	0.0	0.0	2.3	8.9	227.1	204.9	189.6	100.8	2.6	0.0	0.0	736.2
2002/03	13.9	23.0	0.0	0.0	13.4	28.9	507.5	83.5	135.8	25.6	19.2	5.4	856.2
2003/04	34.5	0.0	18.1	0.0	58.3	57.9	212.5	108.5	92.0	32.5	18.5	27.2	660.0
2004/05	27.2	19	0	26	69.7	173.5	64.5	51.7	18.4	27.2	0.0	0.0	477.2
total	12.8	6.2	4.3	20.1	70.6	146.4	214.0	139.7	116.1	33.6	10.6	13.8	788.2

Appendix III, Numerical discretizations

III.1. Discretization Darcy's Law and Richards equation

Figure 26 is a numerical schema of the soil for the unsaturated water flow. Here j is the position and k is the time step. Layer $j=1$ is the layer adjacent to the groundwater. Layer $j=4$ is the layer adjacent to the surface. Layer $j=2$ and $j=3$ are the layers in between. The number of layers in between depend on Δz .

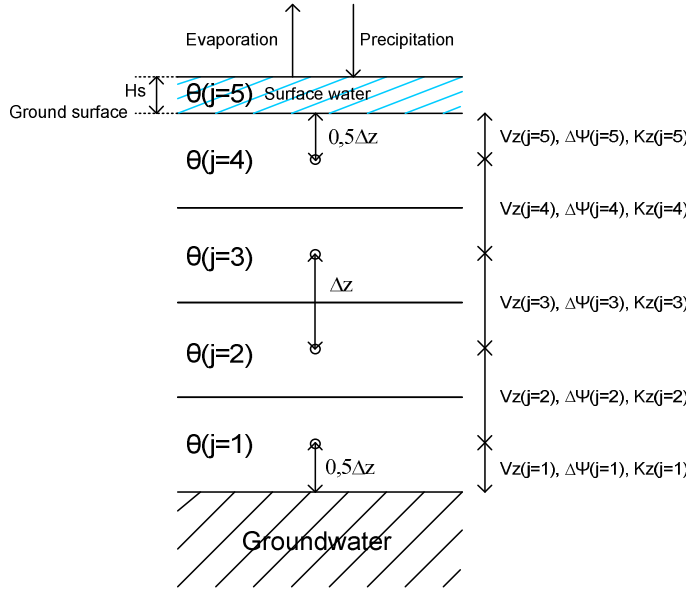


Figure 26, Numerical scheme unsaturated water flow

$$\text{Discretization Darcy's Law, } Vz = K_z(\theta) \frac{\partial \psi(\theta)}{\partial z} - K_z(\theta)$$

$$K_z(j=1, k) = K_z(\theta^{j, k-1})$$

$$K_z(j=2, 3, 4; k) = \frac{2}{\frac{1}{K_z(\theta^{j-1, k-1})} + \frac{1}{K_z(\theta^{j, k-1})}}$$

$$K_z(j=5, k) = K_z(\theta^{j-1, k-1})$$

$$\frac{\partial \psi(j=1, k)}{\partial z} = \frac{\Delta \psi(j)}{0,5\Delta z} = \frac{\psi_{ae} - \psi(\theta^{j, k-1})}{0,5\Delta z}$$

$$\frac{\partial \psi(j=2, 3, 4; k)}{\partial z} = \frac{\Delta \psi(j)}{\Delta z} = \frac{\psi(\theta^{j-1, k-1}) - \psi(\theta^{j, k-1})}{\Delta z}$$

$$\frac{\partial \psi(j=5, k)}{\partial z} = \frac{\Delta \psi(j)}{0,5\Delta z} = \frac{\psi(\theta^{j-1, k-1}) - Hs^{k-1}}{0,5\Delta z}$$

$$Vz(j=1, k) = K_z(\theta^{j, k-1}) \left(\frac{\psi_{ae} - \psi(\theta^{j, k-1})}{0,5\Delta z} \right) - K_z(\theta^{j, k-1})$$

$$V_z(j = 2,3,4;k) = \left(\frac{2}{\frac{1}{K_z(\theta^{j-1,k-1})} + \frac{1}{K_z(\theta^{j,k-1})}} \right) \left(\frac{\psi(\theta^{j-1,k-1}) - \psi(\theta^{j,k-1})}{\Delta z} - 1 \right)$$

$$V_z(j = 5,k) = K_z(\theta^{j-1,k-1}) \left(\frac{\psi(\theta^{j-1,k-1}) - H_s^{k-1}}{0,5.\Delta z} \right) - K_z(\theta^{j-1,k-1})$$

$$H_s^k = H_s^{k-1} + V_z(5).\Delta t - \text{Evaporation}(t) + \text{Precipitation}(t)$$

Discretization Richards Equation, $\frac{\partial \theta}{\partial t} = \frac{\partial V_z}{\partial z}$

$$\frac{\partial \theta}{\partial t} = \frac{\theta^{j,k} - \theta^{j,k-1}}{\Delta t}$$

$$\frac{\partial V_z}{\partial z} = \frac{(V_z(j,k) - V_z(j+1,k))}{\Delta z}$$

$$\theta^{j,k} = \frac{(V_z(j,k) - V_z(j+1,k))}{\Delta z} . \Delta t + \theta^{j,k-1}$$

III.2. Discretization solute movement

Figure 27 is a numerical schema of the soil for the solute movement. Here j is the position and k is the time step. Layer j=1 is the layer adjacent to the groundwater. Layer j=4 is the layer adjacent to the surface. Layer j=2 and j=3 are the layers in between. The number of layers in between depend on Δz .

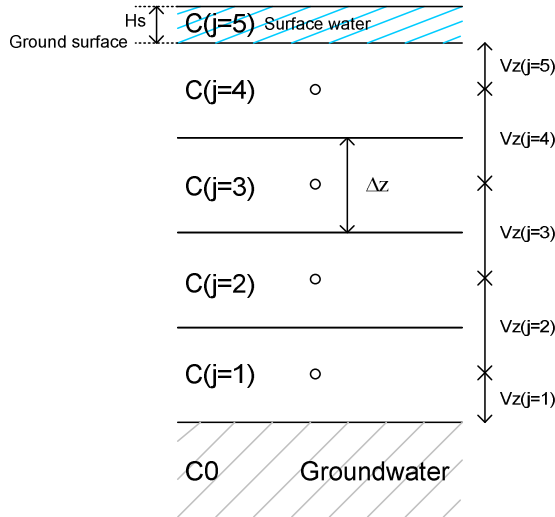


Figure 27, Numerical scheme solute movement

$$\frac{\partial C}{\partial t} = \frac{V_z \partial C}{\partial z}$$

$$\frac{\partial C}{\partial t} = \frac{C^{j,k} - C^{j,k-1}}{\Delta t}$$

$$\frac{V_z \partial C}{\partial z} = \frac{V_z(j)C^{j-1,k-1} - V_z(j+1)C^{j,k-1}}{\Delta z} \text{ if } V_z \text{ is positive}$$

$$\frac{V_z \partial C}{\partial z} = \frac{-V_z(j)C^{j,k-1} + V_z(j+1)C^{j+1,k-1}}{\Delta z} \text{ if } V_z \text{ is negative}$$

$$C^{j,k} = \frac{\left(\frac{V_z(j)C^{j-1,k-1} - V_z(j+1)C^{j,k-1}}{\Delta z} \right) \Delta t + \theta^{j,k-1} C^{j,k-1}}{\theta^{j,k}} \text{ if } V_z \text{ is positive}$$

$$C^{j,k} = \frac{\left(\frac{-V_z(j)C^{j,k-1} + V_z(j+1)C^{j+1,k-1}}{\Delta z} \right) \Delta t + \theta^{j,k-1} C^{j,k-1}}{\theta^{j,k}} \text{ if } V_z \text{ is negative}$$

Because the flux of V_z can either be in or out of the layer with a concentration C , the solute movement has two numerical solutions. If $V_z(j)$ and $V_z(j+1)$ are respectively positive and negative or visa versa the numerical solution becomes a combination of the two solutions. Assumed is that the solute concentration of the groundwater is constant.

Appendix IV, Shortwave and longwave radiation

IV.1.1.1. Shortwave radiation

Shortwave radiation is the radiation from the sun and has wavelengths less than 4 μm . The net shortwave radiation can be determined by the following equation (Dingman 2002):

$$K = K_{in} \cdot (1 - a)$$

K_{in} = incoming shortwave radiation

$$a = \text{albedo watersurface} = 0.127 \cdot \exp(-0.0258 \cdot K_{in})$$

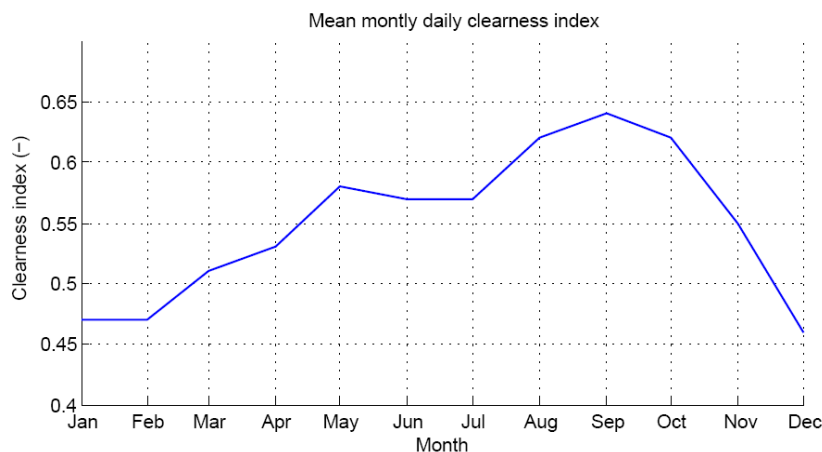
No data of the incoming shortwave radiation available. The shortwave radiation is determined using the monthly mean of the daily clearness index and the monthly mean daily extraterrestrial radiation (Diabaté, Blanc & Wald, 2004):

$$K_{in} = CI \cdot K_0$$

CI = clearness index

K_0 = extraterrestrial radiation

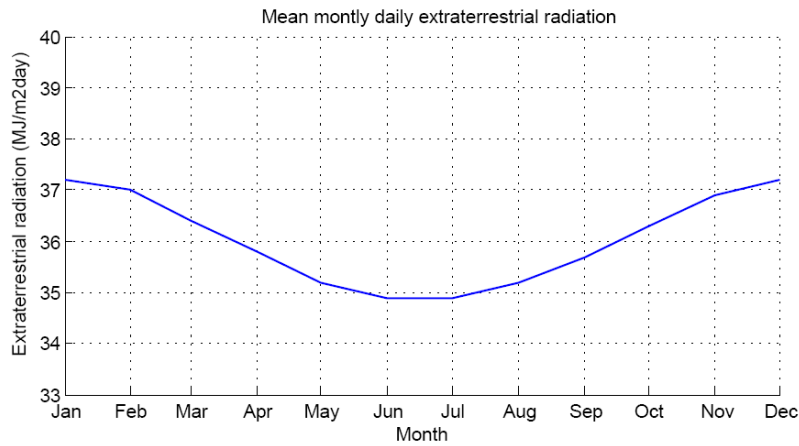
According to Diabaté et al. (2004) the clearness index of Lower Shire Valley ranges from 0.58 to 0.63. Figure 28 is the mean yearly clearness index of the Lower Shire Valley.



month	Clearskyindex (-)
January	0.47
February	0.47
March	0.51
April	0.53
May	0.58
June	0.57
July	0.57
August	0.62
September	0.64
October	0.62
November	0.55
December	0.46

Figure 28, Mean monthly clearness index of the Shire Valley

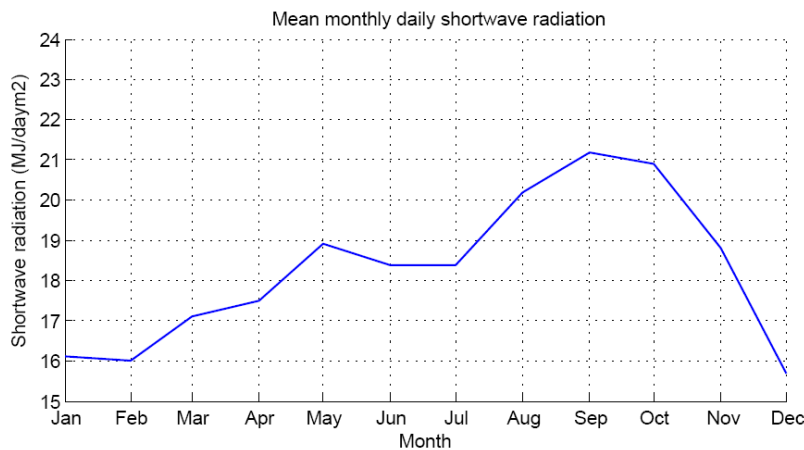
The extraterrestrial radiation is a function of the radiation flux on a plane perpendicular to the solar beam and the angle of the tangent plane relative to the beam (Dingman, 2002). The extraterrestrial radiation is determined by using the SolarRad.xls attached on the CD of physical hydrology (Dingman 2002).



month	Extraterrestrial (MJ/m2day)
January	37.2
February	37.0
March	36.4
April	35.8
May	35.2
June	34.9
July	34.9
August	35.2
September	35.7
October	36.3
November	36.9
December	37.2

Figure 29, Mean monthly daily extraterrestrial radiation of the Shire Valley

Figure 30 holds the total daily net shortwave radiation. The shortwave radiation is the strongest in the months August, September and October.



month	K (MJ/m2day)
January	16.1
February	16.0
March	17.1
April	17.5
May	18.9
June	18.4
July	18.4
August	20.2
September	21.2
October	20.9
November	18.8
December	15.7

Figure 30, Mean monthly daily shortwave radiation of the Shire Valley

IV.1.1.2. Longwave radiation

Longwave radiation is electromagnetic radiation with wavelengths between 4 μm and 20 μm emitted by materials at near-earth-surface temperatures. The net input of longwave radiation can be calculated with the following equations (Dingman, 2002):

$$L = L_{in} - L_{out} = \epsilon_w \cdot \epsilon_{at} \cdot \sigma \cdot (T_a + 273.2)^4 - \epsilon_w \cdot \sigma \cdot (T_s + 273.2)^4$$

$$\epsilon_w = \text{effective emissivity} = 0.95[-]$$

$$\epsilon_{at} = 1.72 \cdot \left(\frac{e_a}{T_a + 273.2} \right)^{1/7} \cdot (1 + 0.22 \cdot C^2)$$

$$e_a = \text{air_vapor_pressure [kPa]}$$

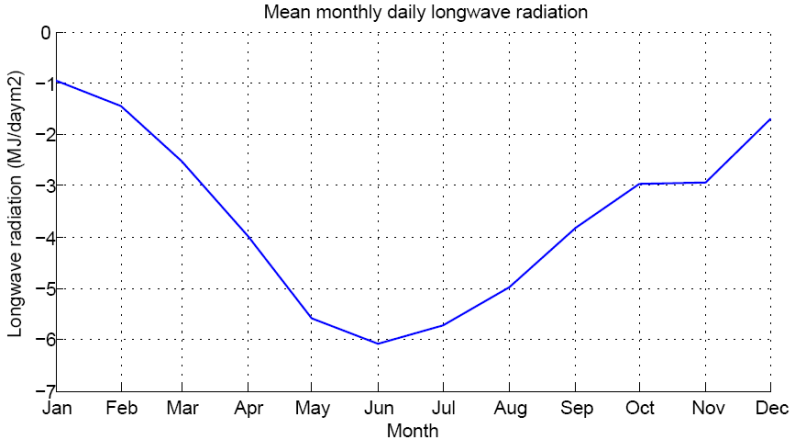
$$e_a = W_a \cdot e_a^*$$

$$T_s = \text{watersurface temperature } e[^\circ\text{C}]$$

$$C = \text{cloud - cover fraction}[-]$$

$$\sigma = \text{Stefan - Boltzmann constant} = 4.90 \cdot 10^{-9} [\text{MJm}^{-2} \text{day}^{-1} \text{K}^{-4}]$$

Data of the water surface temperature and cloud cover fraction can be found in Appendix III. Figure 31 is a plot of the longwave radiation. The longwave radiation is negative through the whole year. Especially in the months May, June and July the net longwave radiation is negative, meaning the surface water emits more electromagnetic radiation than it receives.



Month	L (MJ/m ² day)
January	-0.94
February	-1.46
March	-2.52
April	-3.98
May	-5.58
June	-6.08
July	-5.71
August	-4.98
September	-3.81
October	-2.95
November	-2.94
December	-1.69

Figure 31, Mean monthly daily longwave radiation of the Shire Valley

Appendix V, Results run 3 and 4

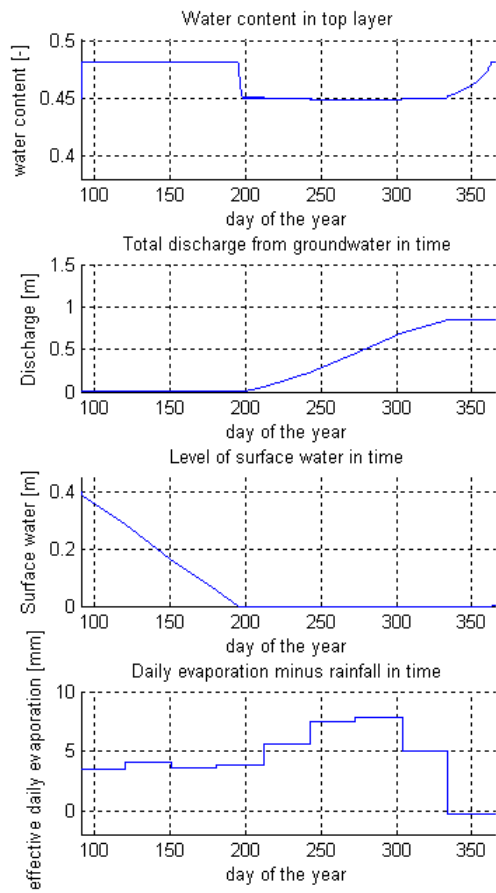


Figure 32, water flow in the unsaturated zone, run 3

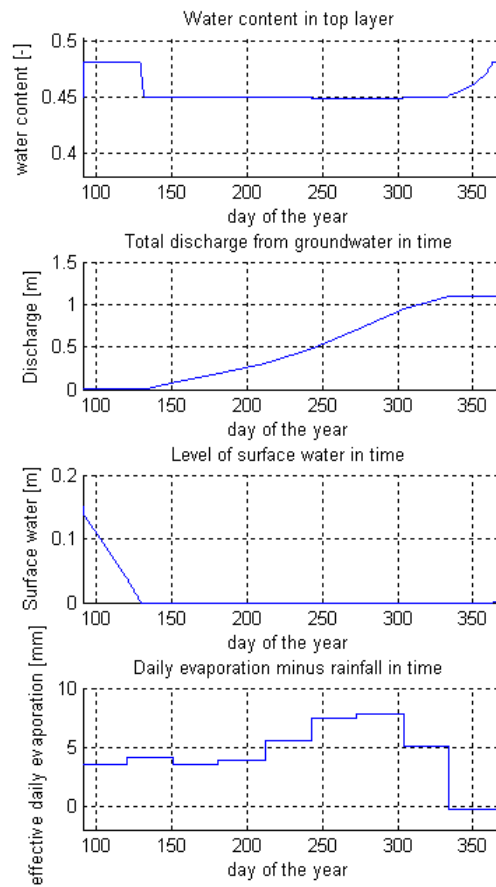


Figure 34, water flow in the unsaturated zone, run 4

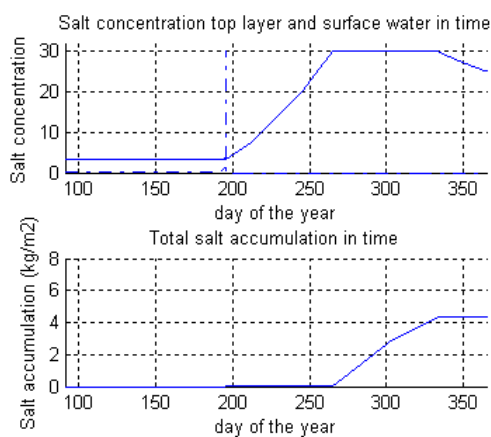


Figure 33, sodium concentration and salt accumulation, run 3

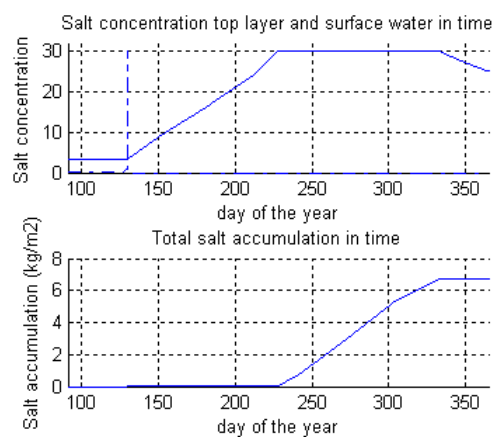


Figure 35, sodium concentration and salt accumulation, run 4

Appendix VI, Matlab script

```

% *****1. Basic parameters *****
dt=0.01;           %time step in days (max 1 of veelfout van 1, min 0.01)
dx=0.125;         %layer width [m] (max z)
start=91;         %the starting day of the modelling, min 1 [day]
einde=365;        %max 365 [day]
a=100;           %Number of days equilibrium run [day]

% *****2. Soil and water properties *****
z=0.5;           %distance groundsurface to groundwater [m]
cground=3.771;   %concentration of Na in the groundwater [g/dm3]
chs=0.015;       %concentration of Na in surface water [g/dm3]
cmax=30;         %maximum concentration of Na in water [g/dm3] in top layer
of dx=0.1m
hs00=0.15;       %amount of surface water [m]

% { % = activated
% { = deactivated, % }

% {
%Sandy clay (table 6-1 Dingman)
khs=0.187;       %saturated hydraulic conductivity [m/dag] (1 cm/s = 864m/dag)
wcmx=0.426;      %porosity [-]
psiae=0.153;     %air entry tension [m]
b=-10.4;        %pore size distribution index [-]
% }

% { %
%Clay (table 6-1 Dingman)
khs=0.111;       %saturated hydraulic conductivity [m/dag] (1 cm/s = 864m/dag)
wcmx=0.482;      %porosity [-]
psiae=0.405;     %air entry tension [m]
b=-11.4;        %pore size distribution index [-]
% }

wcmn= wcmx* (psiae/3.4)^(1/-b); %Field capacity, 33kPa [-]
c= 2+(3/b);      %pore-disconnectedness index [-]
tlength=einde-start; %modelling time in days
timesteps= tlength/dt; %number of time steps
nl= z/dx;        %number of layers
% *****3. Determine effectieve evaporation matrix *****
% { %
ejaar=[];
for n=1:1:12
    for m=((dagenmaand(n)/dt)-(1/dt)+1):1:((dagenmaand(n+1)-1)/dt);
        ejaar(m)=(dt*evaporation(n)/dagenmaand(n+13));
    end
end
end

```

```

rjaar=[];
for n=1:1:12;
    for m=((dagenmaand(n)/dt)-(1/dt)+1):1:((dagenmaand(n+1)-1)/dt);
        rjaar(m)=(dt*rainfall(n)/dagenmaand(n+13));
    end
end
etjaar0=[];
etjaar0=(ejaar-rjaar);

etjaar=[];
for i=(start/dt):1:(einde/dt);
    etjaar(i+1-(start/dt))=etjaar0(i);
end

etequilibrium=[];
etgem= sum(etjaar0)/365;
for i=1:1:(a/dt);
    etequilibrium(i)=etgem*dt;
end

% }
% *****4. Determine equilibrium *****
% { %
layer0=[];
layer0(1,1,1)=wcmax;
for i=1:nl;
    layer0(i+1,1,1)=wcmin+0.05;
end
layer0(nl+2,1,1)=1;

layer0(1,2,1)=cground ;           %Salt concentration ground water
for i=1:nl;
    layer0(i+1,2,1)=cground;       %Salt concentration vadose zone
end
layer0(nl+2,2,1)=chs;             %Salt concentration surface water

psi=[];
kh=[];
kh2=[];
vz=[];

for t=1:1:(a/dt);                 %run of 100 days
    % evaporation
    for i=nl+1;
        layer0(i,1,t)=layer0(i,1,t)-(etequilibrium(t)/(1000*dx));
    end

    %herstel wcmin
    for i=2:1:nl+1
        layer011(i)=((layer0(i,1,t)-wcmin)/(((layer0(i,1,t)-wcmin)^2)^0.5));
    end
end

```

```

end

for i=2:1:nl+1
    layer0(i,1,t)= ((layer011(i)+(layer011(i)^2))/2)*layer0(i,1,t)-((layer011(i)-
(layer011(i)^2))/2)*wcmin;
end

for i=1:1:nl;
    psi(i,1,1)=psiae*((wcmax/layer0(i+1,1,t))^b);
end
for i=1:1:nl;
    kh(i,1,1)=khs*((psiae/psi(i,1,1))^(2+(3/b)));
end

vz(1,1,1)=-kh(1,1,1)*(((psiae-psi(1,1,1))/(0.5*dx))+1);
for i=2:1:nl;
    vz(i,1,1)=-2/(((1/kh(i-1,1,1))+1/kh(i,1,1))))* (((psi(i-1,1,1)-psi(i,1,1))/dx)+1);
end
vz(nl+1,1,1)=0;

for i=1:1:nl;
    layer0(i+1,1,t+1)=layer0(i+1,1,t)+(((vz(i,1,1)-vz(i+1,1,1))/dx)*dt);
end
layer0(1,:,t+1)=layer0(1,:,t);
layer0(nl+2,:,t+1)=layer0(nl+2,:,t);
end

for i=2:nl+1;
    layer0(i,2,end)=cground;
end

layer0(:,end);
% }
% *****5. Simulation *****
% { %
layer2=[];
layer=[];
layer=layer0(:,end);
saltaccumulation=[];
saltaccumulation(1,1)=0;
saltaccumulation(1,2)=0;
hs=[];
hs(1,1,1)=hs00;
hs(1,2,1)=chs;
layer000=[];
capillary=[];
capillary(1)=0;

for t=1:1:((einde-start)/dt);

```

```

%5.1 layers voor berekening salt concentration
layer2=layer(nl+1,1,t);
hs2=hs(1,1,t);

%5.2 evaporation
e00=hs(1,1,t)/(((hs(1,1,t))^2)^0.5);
e000=(e00+(e00^2))*0.5;
e0000=(e00-(e00^2))*-0.5;
for i=nl+1;
    layer(i,1,t)=layer(i,1,t)-((etjaar(t)/(1000*dx))*e0000);
end
for i=nl+2;
    hs(1,1,t)=hs(1,1,t)-((etjaar(t)/1000)*e000);
end

%5.3 watercontent toplayer niet lager dan wmin
for i=2:1:nl+1
    layer(i,1,t)=(((layer(i,1,t)-wmin)/(((layer(i,1,t)-wmin)^2)^0.5)+1)/2)*layer(i,1,t)-
    (((layer(i,1,t)-wmin)/(((layer(i,1,t)-wmin)^2)^0.5)-1)/2)*wmin);
end

%5.4 psi and kh as function of the water content
for i=1:1:nl;
    psi(i,1,1)=psiae*((wmax/layer(i+1,1,t))^b);
end
psi(nl+1,1,1)=-hs(1,1,t)+psiae;
for i=1:1:nl;
    kh(i,1,1)=khs*((psiae/psi(i,1,1))^(2+(3/b)));
end

%5.6 water flux between layers
vz(1,1,1)=-kh(1,1,1)*(((psiae-psi(1,1,1))/(0.5*dx))+1);
for i=2:1:nl;
    vz(i,1,1)=-2/((1/kh(i-1,1,1))+1/kh(i,1,1)))* (((psi(i-1,1,1)-psi(i,1,1))/dx)+1);
end
vz(nl+1,1,1)=-kh(nl,1,1)*(((psi(nl,1,1)-psi(nl+1,1,1))/(0.5*dx))+1);

%5.7 geen flux naar grondwater (already saturated)
vz00000=(vz(1,1,1)/(((vz(1,1,1))^2)^0.5));
vz(1,1,1)=vz(1,1,1)*(vz00000+vz00000^2)*0.5-(10^-60);

%5.8 geen flux naar hs toe of als hs<0
vz0000=hs(1,1,t)/(((hs(1,1,t))^2)^0.5); %1 als hs>0
vz000=(vz(nl+1,1,1)/(((vz(nl+1,1,1))^2)^0.5)); %1 als vz(nl+1) naar boven is gericht
vz(nl+1,1,1)=vz(nl+1,1,1)*-0.25*(vz000-(vz000^2))*(vz0000+(vz0000^2))-(10^-60);

%5.9 water content met herstel om over saturtion te voorkomen!!
for i=1:1:(nl+1);
for i=1:1:nl;
    layer000(i+1,1,t+1)=layer(i+1,1,t)+(((vz(i,1,1)-vz(i+1,1,1))/dx)*dt);

```

```

end
for i=1:1:nl;
    layer11(i)=-((layer000(i+1,1,t+1)-wcmax-(10^-60))/(((layer000(i+1,1,t+1)-wcmax-(10^-60))^2)^0.5));
end
for i=1:1:nl;
    layer(i+1,1,t+1)=0.5*layer000(i+1,1,t+1)*(layer11(i)+(layer11(i)^2))+
0.5*wcmax*(layer11(i)-(layer11(i)^2))-(10^-60);
end

%effective water flow, met verrekening van saturation
for i=1:1:nl;
    vz(i+1)=((layer000(i+1,1,t+1)-layer(i+1,1,t+1))*dx)/dt+vz(i+1)-(10^-60);
end
end

%5.10 nstellen waarden grondwater, en surface water
layer(1,:,t+1)=layer(1,:,t);
hs(1,1,t+1)=hs(1,1,t)+vz(nl+1)*dt;

%5.11 Salt content
%5.11.1 bapalen matrix richting flux
for i=1:1:nl+1;
    vz11(i) = (vz(i)/(((vz(i))^2)^0.5)+((vz(i)/(((vz(i))^2)^0.5))^2))/2;
end

%5.11.2 correctie voor verdamping en oorspronkelijk water content (hoeveelheid zout in top layer)
for i=1:1:nl-1;
    layer(i+1,2,t+1)=((((layer((i+1-vz11(i)),2,t)*vz(i,1,1))-(layer((i+2-vz11(i+1)),2,t)*vz(i+1,1,1)))/dx)*dt)+(layer(i+1,2,t)*layer(i+1,1,t)))/layer(i+1,1,t+1);
end

layer(nl+2,2,t)=hs(1,2,t);
for i=nl;
    layer(i+1,2,t+1)=((((layer((i+1-vz11(i)),2,t)*vz(i,1,1))-(layer((i+2-vz11(i+1)),2,t)*vz(i+1,1,1)))/dx)*dt)+(layer(i+1,2,t)*layer2(1,1,1)))/layer(i+1,1,t+1);
end
hs(1,2,t+1)=(((layer((nl+2-vz11(nl+1)),2,t)*vz(nl+1))*dt)+
(hs2(1,1,1)*hs(1,2,t)))/hs(1,1,t+1);

%5.11.3 salt accumulation
layernl0=layer(nl+1,2,t+1);
layernl11=(-layer(nl+1,2,t+1)+cmax)/(((layer(nl+1,2,t+1)-cmax)^2)^0.5);
layer(nl+1,2,t+1)= -cmax*((layernl11-
(layernl11^2))/2)+layernl0*((layernl11+(layernl11^2))/2);

hs000=hs(1,2,t+1);
hs11= ((-hs(1,2,t+1)+cmax)/(((hs(1,2,t+1)+cmax)^2)^0.5));
hs(1,2,t+1)= -cmax*((hs11-(hs11^2))/2)+hs000*((hs11+(hs11^2))/2);

```

```

hs111=(((hs(1,1,t+1)/((hs(1,1,t+1)^2)^0.5))-1)/-2);
hs(1,2,t+1)=hs(1,2,t+1)*(1-hs111);

%5.11.4 saltaccumulation in kg/m2
saltaccumulation(t+1,1)= (((layernl0-layer(nl+1,2,t+1))*layer(nl+1,1,t+1))*dx*-
1*((layernl11-(layernl11^2))/2)) +saltaccumulation(t,1);
saltaccumulation(t+1,2)= (((hs000-hs(1,2,t+1))*hs(1,1,t+1)*-1*((hs11-(hs11^2))/2)))
+saltaccumulation(t,2);
saltaccumulation(t+1,3)= saltaccumulation(t+1,1)+saltaccumulation(t+1,2);

hs(1,1,t)=hs2;
layer(nl+1,1,t)=layer2;
capillary(t+1)=capillary(t)+vz(1);

end

for i=1:1:(((einde-start)/dt)+1);
layer(nl+1,3,i)=saltaccumulation(i,1)*2.5409;
end

for i=1:1:(((einde-start)/dt)+1);
layer(nl+2,3,i)=saltaccumulation(i,2)*2.5409;
end

for i=1:1:(((einde-start)/dt)+1);
layer(nl+1,4,i)=saltaccumulation(i,3)*2.5409;
end

for i=1:1:(((einde-start)/dt)+1);
layer(nl+2,1,i)=hs(1,1,i);
layer(nl+2,2,i)=hs(1,2,i);
end

layer(:, :, end)

% }

% *****6. Figures *****
% { %
saltc=[];
saltctoplayer=[];
saltcsurface=[];
saltatoplayer=[];
saltasurface=[];
saltatotal=[];

%Salt concentrations
for i=t0;

```

```

saltctoplayer(i)=layer(nl+1,2,i);
end
for i=t0
saltcsurface(i)=layer(nl+2,2,i);
end
for i=t0
saltatoplayer(i)=layer(nl+1,3,i);
end
for i=t0
saltasurface(i)=layer(nl+2,3,i);
end
for i=t0
saltatotal(i)=layer(nl+1,4,i);
end

figure(2*f)
subplot(211)
plot(t, saltctoplayer,'-', 'LineWidth',1)
xlabel('day of the year')
ylabel('Salt concentration')
title('Salt concentration top layer and surface water in time')
axis([91 365 0 32])
box off
grid on
hold
plot(t, saltcsurface,'-', 'LineWidth',1)
hold off
%subplot(312)
%plot(t, saltatoplayer,'-', 'LineWidth',1)
%xlabel('day of the year')
%ylabel('Salt accumulation (kg/m2)')
%title('Salt accumulation top layer in time')
%axis([91 365 0 8 ])
%box off
%grid on
%hold
%plot(t, saltasurface,'-', 'LineWidth',1)
%hold off
subplot(212)
plot(t, saltatotal,'-', 'LineWidth',1)
xlabel('day of the year')
ylabel('Salt accumulation (kg/m2)')
title('Total salt accumulation in time')
axis([91 365 0 8 ])
box off
grid on

% Water content
watercontenttoplayer=[];
surfacewater=[];

```

```

etjaar0=[];

for i=t0;
watercontenttoplayer(i)=layer(nl+1,1,i);
end
for i=t0;
surfacewater(i)=hs(1,1,i);
end
etjaar0=etjaar/dt;
b=wcmin;
a=wcmax;

figure((2*f)-1)
subplot(411)
plot(t, watercontenttoplayer,'-', 'LineWidth',1)
xlabel('day of the year')
ylabel('water content [-]')
title('Water content in top layer')
axis([91 365 (b-0.02) (a+0.02) ])
box off
grid on
subplot(412)
plot(t, (capillary/100),'-', 'LineWidth',1)
xlabel('day of the year')
ylabel('Discharge [m]')
title('Total discharge from groundwater in time')
axis([91 365 0 1.5 ])
box off
grid on
subplot(413)
plot(t, surfacewater,'-', 'LineWidth',1)
xlabel('day of the year')
ylabel('Surface water [m]')
title('Level of surface water in time')
axis([91 365 0 (c+0.05) ])
box off
grid on
subplot(414)
plot(t, etjaar0,'-', 'LineWidth',1)
xlabel('day of the year')
ylabel('effective daily evaporation [mm]')
axis([91 365 -2 10 ])
title('Daily evaporation minus rainfall in time')
box off
grid on
% }

```